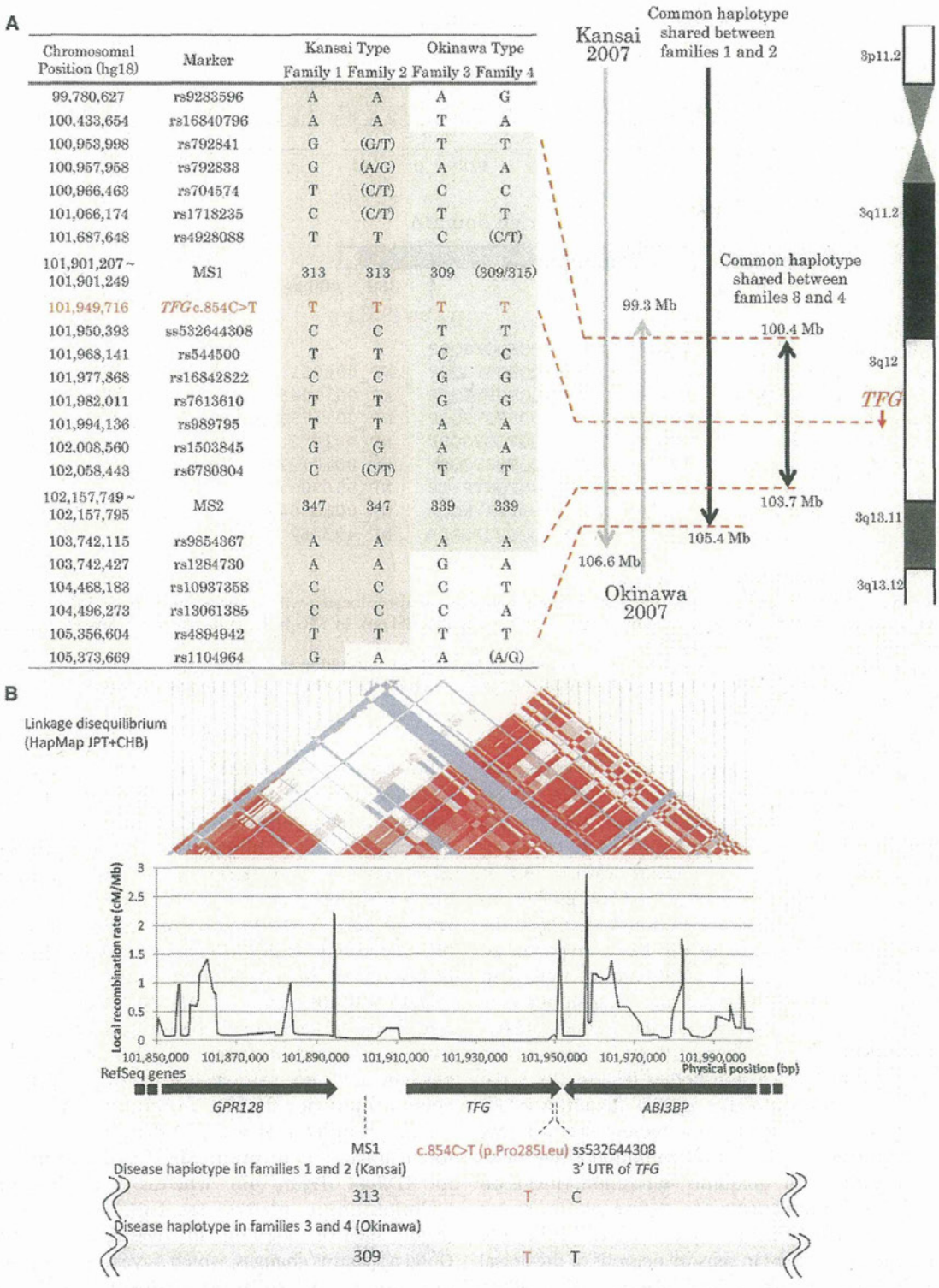

Figure 2. Haplotype Analysis and Minimum Candidate Region of HMSN-P

(A) Haplotypes were reconstructed for all the families with the use of SNP array data and microsatellite markers. Previously reported candidate regions are shown as "Kansai 2007" and "Okinawa 2007."[1,6] Because families 1 and 2 are distantly related, an extended shared common haplotype was observed on chromosome 3, as indicated by a previous study.[6] A reassessment of linkage analysis with high-density SNP markers revealed a recombination between rs4894942 and rs1104964 in family 2, thus refining the telomeric boundary of the candidate region in Kansai families (designated as "Common haplotype shared between families 1 and 2). Furthermore, a shared common haplotype (3.3 Mb with boundaries at rs16840796 and rs1284730) between families 3 and 4 was found, defining the minimum candidate region.

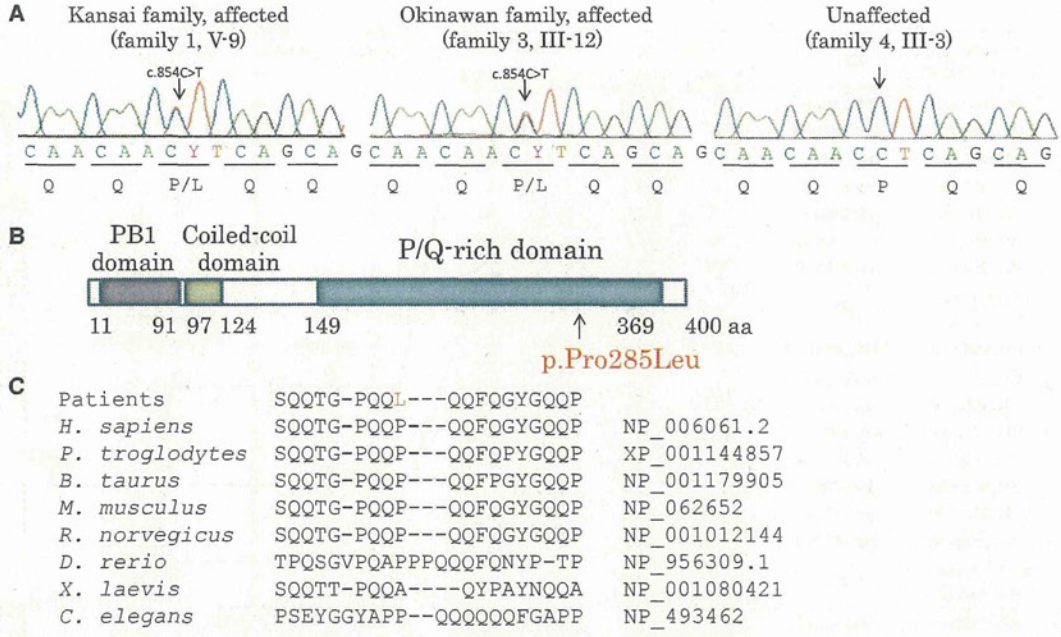

Figure 3. Identification of Causative Mutation

(A) Exome sequencing revealed that only one novel nonsynonymous variant is located within the minimum candidate region. Direct nucleotide-sequence analysis confirmed the mutation, c.854C>T (p.Pro285Leu), in *TFG* in both Kansai and Okinawan families. The mutation cosegregated with the disease (Figure 1A).

(B) Schematic representation of TFG isoform 1. The alteration (p.Pro285Leu) detected in this study is shown below.

(C) Cross-species homology search of the partial TFG amino acid sequence containing the p.Pro285Leu alteration revealed that Pro285 is evolutionally conserved among species.

pneumonia at 67 years of age.[5] Immunohistochemical observations employing a TFG antibody (Table S8) revealed fine granular immunostaining of TFG in the cytoplasm of motor neurons in the spinal cord of neurologically normal controls (n = 3; age at death = 58.7 ± 19.6 years old) (Figure 4A). In the HMSN-P patient, in contrast, TFG-immunopositive inclusion bodies were detected in the motor neurons of the facial, hypoglossal, and abducens nuclei and the spinal cord, as well as in the sensory neurons of the dorsal root ganglia, but were not detected in glial cells (Figures 4B–4D). A small number of cortical neurons in the precentral gyrus also showed TFG-immunopositive inclusion bodies (Figure 4E). Serial sections stained with antibodies against ubiquitin or TFG (Figure 4F) and double immunofluorescence staining (Figure 4G) demonstrated that TFG-immunopositive inclusions colocalized with ubiquitin deposition. Inclusion bodies were immunopositive for optineurin in motor neurons of the brainstem nuclei and the anterior horn of the spinal cord,[5] as well as in sensory neurons of the dorsal root ganglia (data not shown). These data strongly indicate that HMSN-P is a proteinopathy involving TFG.

Because HMSN-P and ALS share some clinical characteristics, we then examined whether neuropathological findings of HMSN-P shared cardinal features with those of sporadic ALS.[13–16] Immunohistochemistry with a TDP-43 antibody revealed skein-like inclusions in the remaining motor neurons of the abducens nucleus and the anterior horn of the lumbar cord (Figures 4H–4I). Phosphorylated TDP-43-positive inclusions were also identified in neurons of the anterior horn of the cervical cord and Clarke's nucleus (Figures 4J–4K). In contrast, TFG immunostaining of spinal-cord specimens from four patients with sporadic ALS (their age at death was 72.3 ± 7.4 years old) revealed no pathological staining in the motor neurons (data not shown). Double immunofluorescence staining revealed that many of the TFG-immunopositive round inclusions in the HSMN-P patient were negative for TDP-43 (Figure 4L), whereas a small number of inclusions were positive for both TFG and TDP-43 (Figure 4M). In addition, to investigate morphological Golgi-apparatus changes, which have recently been found in motor neurons of autopsied tissues of ALS patients,[17] we conducted immunohistochemical analysis by using

(B) Disease haplotypes in the Kansai and Okinawan kindreds are indicated below. Local recombination rates, RefSeq genes, and the linkage disequilibrium map from HapMap JPT (Japanese in Tokyo, Japan) and CHB (Han Chinese in Beijing, China) samples are shown above the disease haplotypes. When disease haplotypes of the Kansai and Okinawan kindreds are compared, the markers nearest to *TFG* are discordant at markers 48.5 kb centromeric and 677 bp telomeric to the mutation within a haploblock, strongly supporting the interpretation that the mutations have independent origins.

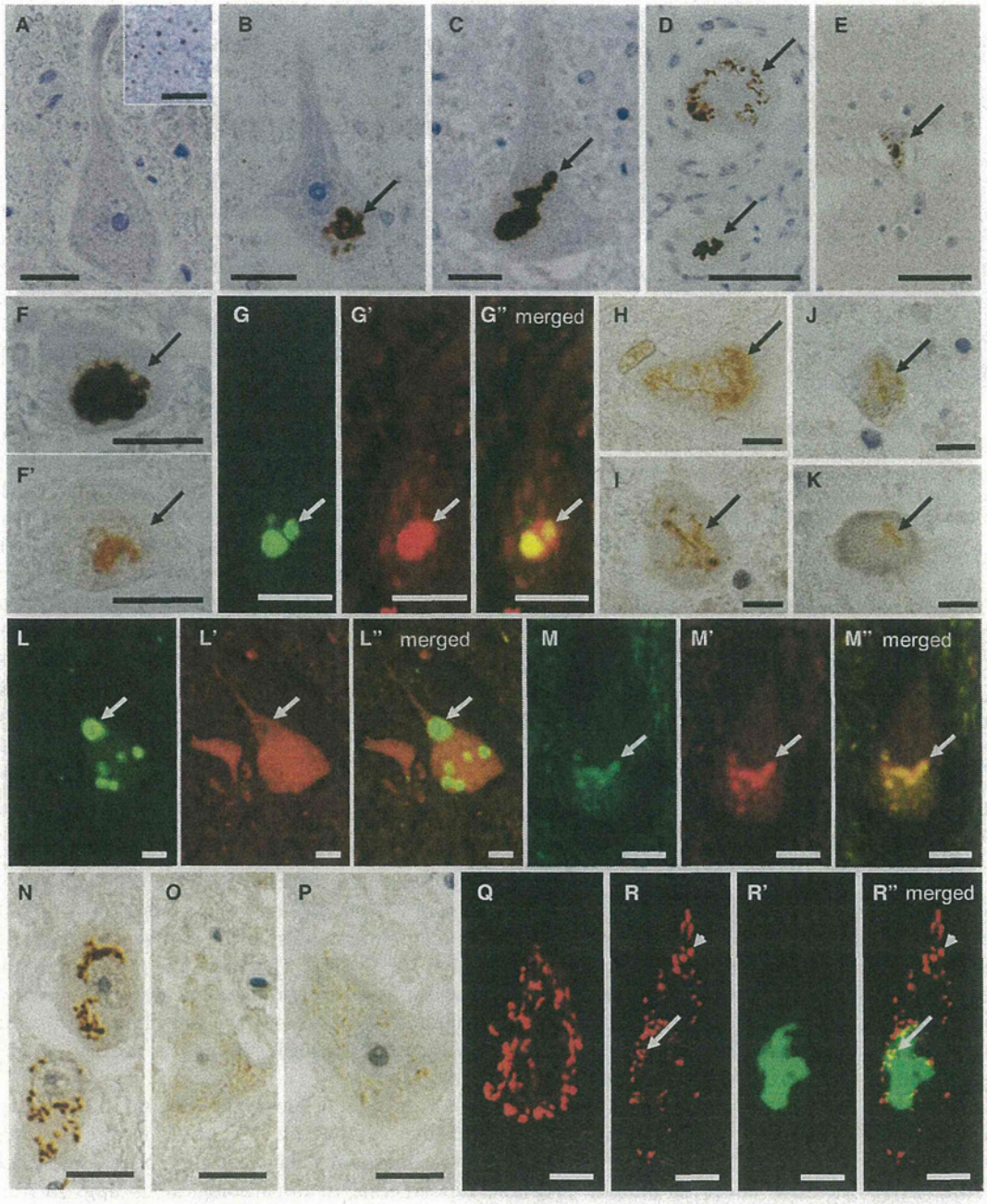

Figure 4. TFG-Related Neuropathological Findings

(A) TFG immunostaining (with hematoxylin counterstaining) of a motor neuron in the spinal cord of a neurologically normal control. A high-power magnified photomicrograph (inset) shows fine granular staining of TFG in the cytoplasm. The scale bars represent 20 μm (main panel) and 10 μm (inset).

(B–E) TFG-immunopositive inclusions of the neurons (with hematoxylin counterstaining) in the hypoglossal nucleus (B), anterior horn of the spinal cord (C), dorsal root ganglion (D, arrows), and motor cortex (E, arrow) of the patient with the *TFG* mutation. The scale bars represent 20 μm (B–D) and 50 μm (E).

(F and F′) Serial section analysis of the facial nucleus motor neuron showing an inclusion body colabeled for TFG (F) and ubiquitin (F′). The scale bars represent 20 μm.

(G–G″) Double immunofluorescence microscopy confirming colocalization of TFG (green) and ubiquitin (red) in an inclusion body of a motor neuron in the hypoglossal nucleus. The scale bars represent 20 μm.

(H and I) TDP-43-positive skein-like inclusions in the motor neurons of the abducens nucleus (H) and anterior horn of the lumbar cord (I). The scale bars represent 20 μm.

(J and K) Phosporylated TDP-43-positive inclusion bodies in the cervical anterior horn (J) and Clarke's nucleus (K). The scale bars represent 20 μm.

(L–L″) Round inclusions (arrows) positive for TFG (green) but negative for TDP-43 (red). The scale bars represent 20 μm.

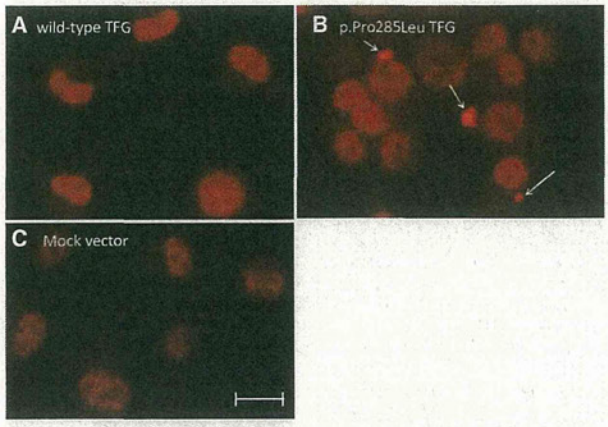

Figure 5. Formation of Cytoplasmic TDP-43 Aggregation Bodies in Cells Stably Expressing Mutant p.Pro285Leu TFG
The coding sequence of *TFG* cDNA was subcloned into pBluescript (Stratagene). After site-directed mutagenesis with a primer pair shown in Table S9, the mutant cDNAs were cloned into the BamHI and XhoI sites of pcDNA3 (Life Technologies). Stable cell lines were established by Lipofectamine (Life Technologies) transfection according to the manufacturer's instructions. Established cell lines were cultured under the ordinary cell-culture conditions (37°C and 5% CO_2) for 5–6 days and were subjected to immunocytochemical analyses. Neuro-2a cells stably expressing wild-type TFG (A), mutant TFG (p.Pro285Leu) (B), and a mock vector (C) are shown. TDP-43-immunopositive cytoplasmic inclusions are absent in the cells stably expressing wild-type TFG or the mock vector (A and C); however, TDP-43-immunopositive cytoplasmic inclusions were exclusively demonstrated in cells stably expressing mutant TFG (p.Pro285Leu), as indicated by arrows (B). Similar results were obtained with HEK 293 cells (not shown). Scale bars represent 10 μm.

a TGN46 antibody. It revealed that the Golgi apparatus was fragmented in approximately 70% of the remaining motor neurons in the lumbar anterior horn. The fragmentation of the Golgi apparatus was prominent near TFG-positive inclusion bodies (Figures 4N–4R). In summary, we found abnormal TDP-43-immunopositive inclusions in the cytoplasm of motor neurons, as well as fragmentation of the Golgi apparatus in HMSN-P, confirming the overlapping neuropathological features between HMSN-P and sporadic ALS.

To further investigate the effect of mutant TFG in cultured cells, stable cell lines expressing wild-type and mutant TFG (p.Pro285Leu) were established from neuro-2a and human embryonic kidney (HEK) 293 cells as previously described.[18] Established cell lines were cultured under the ordinary cell-culture conditions (37°C and 5% CO_2) for 5–6 days and were subjected to immunocytochemical analyses. The neuro-2a cells stably expressing wild-type or mutant TFG demonstrated no distinct difference in the distribution of endogenous TFG, FUS, or OPTN (data not shown). In contrast, cytoplasmic inclusions containing endogenous TDP-43 were exclusively observed in the neuro-2a cells stably expressing untagged mutant TFG, but not in those expressing wild-type TFG (Figure 5). Similar data were obtained from HEK 293 cells (data not shown). Thus, the expression of mutant TFG leads to mislocalization and inclusion-body formation of TDP-43 in cultured cells.

TFG was originally identified as a part of fusion oncoproteins (NTRK1-T3 in papillary thyroid carcinoma,[19] TFG-ALK in anaplastic large cell lymphoma,[20] and TFG/NOR1 in extraskeletal myxoid chondrosarcoma[21]), where the N-terminal portions of TFG are fused to the C terminus of tyrosine kinases or a superfamily of steroid-thyroid hormone-retinoid receptors acting as a transcriptional activator leading to the formation of oncogenic products. Very recently, TFG-1, a homolog of TFG in *Caenorhabditis elegans*, and TFG have been discovered to localize in endoplasmic-reticulum exit sites. TFG-1 acts in a hexameric form that binds the scaffolding protein Sec16 complex assembly and plays an important role in protein secretion with COPII-coated vesicles.[22] It is noteworthy that mutations in genes involved in vesicle trafficking[23,24] (such genes include *VAPB*, *CHMP2B*, *alsin*, *FIG4*, *VPS33B*, *PIP5K1C*, and *ERBB3*) cause motor neuron diseases, emphasizing the role of vesicle trafficking in motor neuron diseases. Thus, altered vesicle trafficking due to the *TFG* mutation might be involved in the motor neuron degeneration in HMSN-P. The presence of TFG-immunopositive inclusions in motor neurons raises the possibility that mutant TFG results in the misfolding and formation of cytoplasmic aggregate bodies, as well as altered vesicle trafficking.

An intriguing neuropathological finding is TDP-43-positive cytoplasmic inclusions in the motor neurons; these inclusions have recently been established as the fundamental neuropathological findings in ALS.[13,14] Of note, expression of mutant, but not wild-type, TFG in cultured cells led to the formation of TDP-43-containing cytoplasmic aggregation. These observations are similar

(M–M″) An inclusion immunopositive for both TFG (green) and TDP-43 (red) is observed in a small number of neurons. The scale bars represent 20 μm.
(N) Normal Golgi apparatus in the neurons of the intact thoracic intermediolateral nucleus. The scale bar represents 20 μm.
(O and P) Fragmentation of the Golgi apparatus with small, round, and disconnected profiles in the affected motor neurons of the lumbar anterior horn. The scale bars represent 20 μm.
(Q–R″) Immunohistochemical observations of the Golgi apparatus and TFG-immunopositive inclusions employing antibodies against TGN46 (red) and TFG (green), respectively. The scale bars represent 10 μm.
(Q) Normal size and distribution (red) in a motor neuron without inclusions.
(R–R″) The Golgi apparatus was fragmented into various sizes and reduced in number in the lumbar anterior horn motor neuron with TFG-positive inclusions (green). The fragmentation predominates near the inclusion (arrow), whereas the Golgi apparatuses distant from the inclusion showed nearly normal patterns (arrow head).

to what has been described for ALS, where TDP-43 is mislocalized from the normally localized nucleus to the cytoplasm with concomitant cytoplasmic inclusions. Cytoplasmic TDP-43 accumulation and inclusion formation have also been observed in motor neurons in familial ALS with mutations in *VAPB* (MIM 608627) or *CHMP2B* (MIM 600795).[25,26] Furthermore, TDP-43 pathology has been demonstrated in transgenic mice expressing mutant VAPB.[27] Although the mechanisms of mislocalization of TDP-43 remain to be elucidated, these observations suggest connections between alteration of vesicle trafficking and mislocalization of TDP-43. Thus, common pathophysiologic mechanisms might underlie motor neuron degenerations involving vesicle trafficking including TFG, as well as VAPB and CHMP2B. Because TDP-43 is an RNA-binding protein, RNA dysregulation has been suggested to play important roles in the TDP43-mediated neurodegeneration.[28] Furthermore, recent discovery of hexanucleotide repeat expansions in *C9ORF72* in familial and sporadic ALS/FTD (MIM 105550)[29,30] emphasizes the RNA-mediated toxicities as the causal mechanisms of neurodegeneration. Observations of TDP-43-positive cytoplasmic inclusions in the motor neurons of the patient with HMSN-P raise the possibility that RNA-mediated mechanisms might also be involved in motor neuron degeneration in HMSN-P.

In summary, we have found that *TFG* mutations cause HMSN-P. The presence of TFG/ubiquitin- and/or TDP-43-immunopositive cytoplasmic inclusions in motor neurons and cytosolic aggregation composed of TDP-43 in cultured cells expressing mutant TFG indicate a novel pathway of motor neuron death.

Supplemental Data

Supplemental Data include three figures and nine tables and can be found with this article online at http://www.cell.com/AJHG/.

Acknowledgments

The authors thank the families for participating in the study. We also thank the doctors who obtained clinical information of the patients. This work was supported in part by Grants-in-Aid for Scientific Research on Innovative Areas (22129002); the Global Centers of Excellence Program; the Integrated Database Project; Scientific Research (A) (B21406026) and Challenging Exploratory Research (23659458) from the Ministry of Education, Culture, Sports, Science, and Technology of Japan; a Grant-in-Aid for Research on Intractable Diseases and Comprehensive Research on Disability Health and Welfare from the Ministry of Health, Labour, and Welfare, Japan; Grants-in-Aid from the Research Committee of CNS Degenerative Diseases; the Ministry of Health, Labour, and Welfare of Japan; the Charcot-Marie-Tooth Association; and the National Medical Research Council of Australia. H.I. was supported by a Research Fellowship from the Japan Society for the Promotion of Science for Young Scientists. We also thank S. Ogawa (Cancer Genomics Project, The University of Tokyo) for his kind help in the analyses employing GAIIx and SOLiD4.

Received: April 16, 2012
Revised: May 27, 2012
Accepted: July 2, 2012
Published online: August 9, 2012

Web Resources

The URLs for data presented herein are as follows.

1000 Genomes Project Database, http://www.1000genomes.org/
dbSNP, http://www.ncbi.nlm.nih.gov/projects/SNP/
HapMap, http://hapmap.ncbi.nlm.nih.gov/
NHLBI GO Exome Sequencing Project, https://esp.gs.washington.edu/drupal/
Online Mendelian Inheritance in Man (OMIM), http://www.omim.org
PolyPhen, http://genetics.bwh.harvard.edu/pph/
RefSeq, http://www.ncbi.nlm.nih.gov/projects/RefSeq/
UCSC Human Genome Browser, http://genome.ucsc.edu/

References

1. Takashima, H., Nakagawa, M., Nakahara, K., Suehara, M., Matsuzaki, T., Higuchi, I., Higa, H., Arimura, K., Iwamasa, T., Izumo, S., and Osame, M. (1997). A new type of hereditary motor and sensory neuropathy linked to chromosome 3. Ann. Neurol. *41*, 771–780.
2. Nakagawa, M. (2009). [Wide spectrum of hereditary motor sensory neuropathy (HMSN)]. Rinsho Shinkeigaku *49*, 950–952.
3. Maeda, K., Sugiura, M., Kato, H., Sanada, M., Kawai, H., and Yasuda, H. (2007). Hereditary motor and sensory neuropathy (proximal dominant form, HMSN-P) among Brazilians of Japanese ancestry. Clin. Neurol. Neurosurg. *109*, 830–832.
4. Patroclo, C.B., Lino, A.M., Marchiori, P.E., Brotto, M.W., and Hirata, M.T. (2009). Autosomal dominant HMSN with proximal involvement: new Brazilian cases. Arq. Neuropsiquiatr. *67* (3B), 892–896.
5. Fujita, K., Yoshida, M., Sako, W., Maeda, K., Hashizume, Y., Goto, S., Sobue, G., Izumi, Y., and Kaji, R. (2011). Brainstem and spinal cord motor neuron involvement with optineurin inclusions in proximal-dominant hereditary motor and sensory neuropathy. J. Neurol. Neurosurg. Psychiatry *82*, 1402–1403.
6. Takahashi, H., Makifuchi, T., Nakano, R., Sato, S., Inuzuka, T., Sakimura, K., Mishina, M., Honma, Y., Tsuji, S., and Ikuta, F. (1994). Familial amyotrophic lateral sclerosis with a mutation in the Cu/Zn superoxide dismutase gene. Acta Neuropathol. *88*, 185–188.
7. Maeda, K., Kaji, R., Yasuno, K., Jambaldorj, J., Nodera, H., Takashima, H., Nakagawa, M., Makino, S., and Tamiya, G. (2007). Refinement of a locus for autosomal dominant hereditary motor and sensory neuropathy with proximal dominancy (HMSN-P) and genetic heterogeneity. J. Hum. Genet. *52*, 907–914.
8. Fukuda, Y., Nakahara, Y., Date, H., Takahashi, Y., Goto, J., Miyashita, A., Kuwano, R., Adachi, H., Nakamura, E., and Tsuji, S. (2009). SNP HiTLink: A high-throughput linkage analysis system employing dense SNP data. BMC Bioinformatics *10*, 121.
9. Gudbjartsson, D.F., Thorvaldsson, T., Kong, A., Gunnarsson, G., and Ingolfsdottir, A. (2005). Allegro version 2. Nat. Genet. *37*, 1015–1016.

10. Li, H., and Durbin, R. (2009). Fast and accurate short read alignment with Burrows-Wheeler transform. Bioinformatics *25*, 1754–1760.
11. Li, H., Handsaker, B., Wysoker, A., Fennell, T., Ruan, J., Homer, N., Marth, G., Abecasis, G., and Durbin, R.; 1000 Genome Project Data Processing Subgroup. (2009). The Sequence Alignment/Map format and SAMtools. Bioinformatics *25*, 2078–2079.
12. Robinson, J.T., Thorvaldsdóttir, H., Winckler, W., Guttman, M., Lander, E.S., Getz, G., and Mesirov, J.P. (2011). Integrative genomics viewer. Nat. Biotechnol. *29*, 24–26.
13. Neumann, M., Sampathu, D.M., Kwong, L.K., Truax, A.C., Micsenyi, M.C., Chou, T.T., Bruce, J., Schuck, T., Grossman, M., Clark, C.M., et al. (2006). Ubiquitinated TDP-43 in frontotemporal lobar degeneration and amyotrophic lateral sclerosis. Science *314*, 130–133.
14. Arai, T., Hasegawa, M., Akiyama, H., Ikeda, K., Nonaka, T., Mori, H., Mann, D., Tsuchiya, K., Yoshida, M., Hashizume, Y., and Oda, T. (2006). TDP-43 is a component of ubiquitin-positive tau-negative inclusions in frontotemporal lobar degeneration and amyotrophic lateral sclerosis. Biochem. Biophys. Res. Commun. *351*, 602–611.
15. Hasegawa, M., Arai, T., Nonaka, T., Kametani, F., Yoshida, M., Hashizume, Y., Beach, T.G., Buratti, E., Baralle, F., Morita, M., et al. (2008). Phosphorylated TDP-43 in frontotemporal lobar degeneration and amyotrophic lateral sclerosis. Ann. Neurol. *64*, 60–70.
16. Inukai, Y., Nonaka, T., Arai, T., Yoshida, M., Hashizume, Y., Beach, T.G., Buratti, E., Baralle, F.E., Akiyama, H., Hisanaga, S., and Hasegawa, M. (2008). Abnormal phosphorylation of Ser409/410 of TDP-43 in FTLD-U and ALS. FEBS Lett. *582*, 2899–2904.
17. Stieber, A., Chen, Y., Wei, S., Mourelatos, Z., Gonatas, J., Okamoto, K., and Gonatas, N.K. (1998). The fragmented neuronal Golgi apparatus in amyotrophic lateral sclerosis includes the trans-Golgi-network: Functional implications. Acta Neuropathol. *95*, 245–253.
18. Kuroda, Y., Sako, W., Goto, S., Sawada, T., Uchida, D., Izumi, Y., Takahashi, T., Kagawa, N., Matsumoto, M., Matsumoto, M., et al. (2012). Parkin interacts with Klokin1 for mitochondrial import and maintenance of membrane potential. Hum. Mol. Genet. *21*, 991–1003.
19. Greco, A., Mariani, C., Miranda, C., Lupas, A., Pagliardini, S., Pomati, M., and Pierotti, M.A. (1995). The DNA rearrangement that generates the TRK-T3 oncogene involves a novel gene on chromosome 3 whose product has a potential coiled-coil domain. Mol. Cell. Biol. *15*, 6118–6127.
20. Hernández, L., Pinyol, M., Hernández, S., Beà, S., Pulford, K., Rosenwald, A., Lamant, L., Falini, B., Ott, G., Mason, D.Y., et al. (1999). TRK-fused gene (TFG) is a new partner of ALK in anaplastic large cell lymphoma producing two structurally different TFG-ALK translocations. Blood *94*, 3265–3268.
21. Hisaoka, M., Ishida, T., Imamura, T., and Hashimoto, H. (2004). TFG is a novel fusion partner of NOR1 in extraskeletal myxoid chondrosarcoma. Genes Chromosomes Cancer *40*, 325–328.
22. Witte, K., Schuh, A.L., Hegermann, J., Sarkeshik, A., Mayers, J.R., Schwarze, K., Yates, J.R., 3rd, Eimer, S., and Audhya, A. (2011). TFG-1 function in protein secretion and oncogenesis. Nat. Cell Biol. *13*, 550–558.
23. Dion, P.A., Daoud, H., and Rouleau, G.A. (2009). Genetics of motor neuron disorders: New insights into pathogenic mechanisms. Nat. Rev. Genet. *10*, 769–782.
24. Andersen, P.M., and Al-Chalabi, A. (2011). Clinical genetics of amyotrophic lateral sclerosis: What do we really know? Nat Rev Neurol *7*, 603–615.
25. Ince, P.G., Highley, J.R., Kirby, J., Wharton, S.B., Takahashi, H., Strong, M.J., and Shaw, P.J. (2011). Molecular pathology and genetic advances in amyotrophic lateral sclerosis: an emerging molecular pathway and the significance of glial pathology. Acta Neuropathol. *122*, 657–671.
26. Cox, L.E., Ferraiuolo, L., Goodall, E.F., Heath, P.R., Higginbottom, A., Mortiboys, H., Hollinger, H.C., Hartley, J.A., Brockington, A., Burness, C.E., et al. (2010). Mutations in CHMP2B in lower motor neuron predominant amyotrophic lateral sclerosis (ALS). PLoS ONE *5*, e9872.
27. Tudor, E.L., Galtrey, C.M., Perkinton, M.S., Lau, K.-F., De Vos, K.J., Mitchell, J.C., Ackerley, S., Hortobágyi, T., Vámos, E., Leigh, P.N., et al. (2010). Amyotrophic lateral sclerosis mutant vesicle-associated membrane protein-associated protein-B transgenic mice develop TAR-DNA-binding protein-43 pathology. Neuroscience *167*, 774–785.
28. Lee, E.B., Lee, V.M., and Trojanowski, J.Q. (2012). Gains or losses: Molecular mechanisms of TDP43-mediated neurodegeneration. Nat. Rev. Neurosci. *13*, 38–50.
29. DeJesus-Hernandez, M., Mackenzie, I.R., Boeve, B.F., Boxer, A.L., Baker, M., Rutherford, N.J., Nicholson, A.M., Finch, N.A., Flynn, H., Adamson, J., et al. (2011). Expanded GGGGCC hexanucleotide repeat in noncoding region of C9ORF72 causes chromosome 9p-linked FTD and ALS. Neuron *72*, 245–256.
30. Renton, A.E., Majounie, E., Waite, A., Simón-Sánchez, J., Rollinson, S., Gibbs, J.R., Schymick, J.C., Laaksovirta, H., van Swieten, J.C., Myllykangas, L., et al; ITALSGEN Consortium. (2011). A hexanucleotide repeat expansion in C9ORF72 is the cause of chromosome 9p21-linked ALS-FTD. Neuron *72*, 257–268.

A homozygous mutation of *C12orf65* causes spastic paraplegia with optic atrophy and neuropathy (SPG55)

Haruo Shimazaki,[1] Yoshihisa Takiyama,[2] Hiroyuki Ishiura,[3] Chika Sakai,[4] Yuichi Matsushima,[4] Hideyuki Hatakeyama,[4] Junko Honda,[1] Kumi Sakoe,[1] Tametou Naoi,[1] Michito Namekawa,[1] Yoko Fukuda,[3] Yuji Takahashi,[3] Jun Goto,[3] Shoji Tsuji,[3] Yu-ichi Goto,[4] Imaharu Nakano,[1] and Japan Spastic Paraplegia Research Consortium (JASPAC)

[1]Division of Neurology, Department of Internal Medicine, Jichi Medical University, Tochigi, Japan
[2]Department of Neurology, Interdisciplinary Graduate School of Medicine and Engineering, University of Yamanashi, Yamanashi, Japan
[3]Department of Neurology, Graduate School of Medicine, University of Tokyo, Tokyo, Japan
[4]Department of Mental Retardation and Birth Defect Research, National Institute of Neuroscience, National Center of Neurology and Psychiatry, Tokyo, Japan

Correspondence to
Dr Yoshihisa Takiyama, Department of Neurology, Interdisciplinary Graduate School of Medicine and Engineering, University of Yamanashi, 1110 Shimokato, Chuo-shi, Yamanashi 409-3898, Japan; ytakiyama@yamanashi.ac.jp

Received 11 August 2012
Revised 27 September 2012
Accepted 5 October 2012

ABSTRACT

Background Autosomal recessive hereditary spastic paraplegias (AR-HSP) constitute a heterogeneous group of neurodegenerative diseases involving pyramidal tracts dysfunction. The genes responsible for many types of AR-HSPs remain unknown. We attempted to identify the gene responsible for AR-HSP with optic atrophy and neuropathy.

Methods The present study involved two patients in a consanguineous Japanese family. Neurologic examination and DNA analysis were performed for both patients, and a skin biopsy for one. We performed genome-wide linkage analysis involving single nucleotide polymorphism arrays, copy-number variation analysis, and exome sequencing. To clarify the mitochondrial functional alteration resulting from the identified mutation, we performed immunoblot analysis, mitochondrial protein synthesis assaying, blue native polyacrylamide gel electrophoresis (BN-PAGE) analysis, and respiratory enzyme activity assaying of cultured fibroblasts of the patient and a control.

Results We identified a homozygous nonsense mutation (c.394C>T, p.R132X) in *C12orf65* in the two patients in this family. This *C12orf65* mutation was not found in 74 Japanese AR-HSP index patients without any mutations in previously known HSP genes. This mutation resulted in marked reduction of mitochondrial protein synthesis, followed by functional and structural defects in respiratory complexes I and IV.

Conclusions This novel nonsense mutation in *C12orf65* could cause AR-HSP with optic atrophy and neuropathy, resulting in a premature stop codon. The truncated *C12orf65* protein must lead to a defect in mitochondrial protein synthesis and a reduction in the respiratory complex enzyme activity. Thus, dysfunction of mitochondrial translation could be one of the pathogenic mechanisms underlying HSPs.

INTRODUCTION

Hereditary spastic paraplegias (HSPs) comprise a large and heterogeneous group of genetic disorders mainly affecting the pyramidal tracts of the legs. The cardinal pathological findings in HSPs are the result of a dying back degeneration of the corticospinal tracts in the spinal cord. The longest fibres, innervating the lower extremities are mostly affected. HSPs are divided into two subtypes that comprise pure and complex forms. The pure form of HSP is characterised by progressive bilateral leg spasticity, weakness, exaggerated tendon reflexes and positive pathological reflexes, whereas the complex form of HSP shows the following additional symptoms: peripheral neuropathy, cerebellar atrophy, thin corpus callosum, optic atrophy, retinal degeneration, mental impairment, convulsions and extrapyramidal signs.[1]

HSPs can be inherited in an autosomal-dominant (AD), autosomal-recessive (AR) or X-linked recessive (XR) manner. To date, at least 52 spastic paraplegia gene (SPG) loci have been assigned, and approximately 30 genes have been identified. The pure form is usually transmitted as an AD trait, whereas the complex form is transmitted as an AR or XR one. The most common AD-HSP is SPG4 with the *spastin* gene mutation, accounting for 40–45% of AD-HSP.[2] Meanwhile, the most frequent AR-HSP might be SPG11 with the *spatacsin* gene mutation, showing a complex phenotype including dementia and thin corpus callosum.[3] The genes most responsible for AR-HSPs, however, remain unknown.

Several pathogenic mechanisms underlying HSPs have been suggested. HSPs might result from disruption of the axonal transport of molecules, organelles and other cargos, which mainly affects the distal parts of motor neurones.[4] Axonal transport might be impaired by mutations of the *SPAST* gene[5] and kinesin heavy chain *KIF5A*.[6] An animal model of spastin deletion shows progressive axonal degeneration restricted to the central nervous system leading to a late and mild motor defect. The degenerative process is characterised by focal axonal swelling associated with abnormal accumulation of organelles and cytoskeletal components.[7] The intracellular transport of molecules and organelles to and from nerve terminals also depends on the mitochondrial function.

An abnormal mitochondrial function also leads to several HSPs: SPG7 with the *paraplegin* gene mutation and SPG13 with the heat-shock protein 60 (*HSPD1*) one. For instance, paraplegin is a part of the metalo-protease AAA (ATPases associated with diverse cellular activities) complex with AFG3L2,[8] an ATP-dependent proteolytic complex located at the mitochondrial inner membrane, which controls protein quality and regulates ribosome assembly.[9] A homozygous mutation of *AFG3L2* also leads to spastic ataxia-neuropathy syndrome (SPAX-5 in OMIM).[10] Paraplegin-deficient mice are affected by distal axonopathy of spinal and peripheral axons, characterised by axonal swelling and degeneration caused by

massive accumulation of organelles and neurofilaments, similar to those observed in the animal model of spastin deletion.[11]

Here, we report a novel homozygous nonsense mutation in the chromosome 12 open reading frame 65 (*C12orf65*) gene in patients with AR-HSP with optic atrophy and neuropathy found on linkage analysis involving single nucleotide polymorphism (SNP) and exome sequencing. Furthermore, we revealed that this mutation led to a mitochondrial translation dysfunction in a patient (proband). This is the first report that a *C12orf65* mutation causes HSP.

PATIENTS AND METHODS

Patients

The present study involved two patients from a family with spastic paraplegia, optic atrophy and peripheral neuropathy described elsewhere.[12] The family pedigree is shown in figure 1A. The parents were first cousins. Two affected (IV-3 and 6) and three unaffected members (III-1, 2 and IV-4) of the family underwent neurological examinations and nerve conduction studies, except for III-2 and IV-4.[12] Presently, the unaffected members are all deceased.

Linkage analysis

Genomic DNA was extracted from blood samples from the two affected individuals (IV-3 and 6) with written informed consent (figure 1A), and then multipoint parametric linkage analysis involving a SNP high-throughput linkage analysis system (SNP HiTLink) was performed.[13] With this system, SNP chip data for the Mapping 100 k/500 k array set and Genome-Wide Human SNP array 6.0 (Affymetrix, Santa Clara, California, USA) can be directly imported and passed to a multipoint parametric linkage analysis programme Allegro.[14] Parametric LOD scores were calculated using Allegro V.2 with the parameter setting of an AR model with 100% penetrance.

Copy-number variation detection

We performed array-based comparative genomic hybridisation (aCGH) analysis for copy-number alteration detection in the candidate gene areas. We developed custom aCGH arrays against the candidate areas in the four chromosomes using a Human Genome CGH Microarray Kit 244K (Agilent Technologies, Santa Clara, California, USA) according to the manufacturer's protocol.[15 16] We made one CGH probe every 160 bp on average against the candidate gene areas.

Exome sequencing

We collected a blood sample from one affected individual (IV-6) and performed massively parallel sequencing. Genomic DNA was extracted from leukocytes from the case and then sheared. An adaptor-ligated library was prepared and clustered on the cBOT system (Illumina, San Diego, California, USA). Exon capture was performed with a SureSelect Human All Exon kit (Agilent). Paired-end sequencing was carried out on an Illumina Hiseq 2000 that generated 91-bp reads. For sequence alignment, variant calling and annotation, the sequences were aligned with the human genome reference sequence (hg19 build) using a Burrows-Wheeler Aligner. Substitution calling was carried out with a Genome analysis tool kit (GATK). SNP calls were made with a GATK Unified Genotyper, and indel calls were made with a GATK IndelGenotyper V2. SNP calling was performed with reference to dbSNP131 and dbSNP134. All variants were annotated with reference to consensus coding sequences (CCDS) (NCBI release 20090902) and RefSeq (UCSC dumped 20101004).

Sanger sequencing

The coding exons and flanking intronic sequences of *C12orf65* were amplified using the genomic DNA of the patients, and using an Marshall Scientific (MS) Research Thermal Cycler. The primer sequences were as follows: Ex2-F: aac atg gca gac agt gca ag, Ex2-R: ggc tga tcc cat tca cac tt, Ex3-F: ttc tga ggt cct gtc cat ttt t, and Ex3-R: gcc cag ccg agt ttt att ct. Sanger sequencing was performed according to an established standard protocol on an Applied Biosystems (ABI) 3730 capillary sequencer (Applied Biosystems, Carlsbad, California, USA). We sought additional *C12orf65* mutations by Sanger sequencing of the coding regions of two exons and their flanking sequences of *C12orf65* in 74 index Japanese AR-HSP patients without known HSP gene (SPG1/2/3A/4/5/6/7/8/10/11/13/17/20/21/31/33) substitutions established by the Japan Spastic Paraplegia Research Consortium, and one case in a family with Charcot–Marie–Tooth disease (CMT) and optic atrophy with AR transmission. Genomic DNA samples from 200 Japanese subjects without apparent neurologic disorders were also analysed as controls.

Immunoblotting

Mitochondria were isolated from primary fibloblasts from the patient and two controls. Mitochondrial protein (10 µg per lane) was fractionated by 12% NuPAGE Gel (Life Technologies) and transferred to polyvinylidene fluoride (PVDF) membranes. The filters were preincubated for 1 h with Block One (Nacalai), followed by incubation for 1 h with Can Get Signal solution 1 (Toyobo) containing C12orf65 antibodies (Abcam) or voltage dependent anion channel (VDAC) antibodies (MitoSciences). The filters were washed four times with phosphate-buffered saline (PBS) containing 0.1% Tween 20, incubated for 1 h with Can Get Signal solution 2 (Toyobo) containing horseradish peroxidase-conjugated antirabbit or mouse immunoglobuline G (igG) (GE Healthcare), and then washed with PBS containing 0.1% Tween 20. Protein bands were visualised using enhanced chemiluminescence (ECL) prime western blotting reagents (GE Healthcare).

Mitochondrial protein synthesis assaying[17]

The patient's (IV-6) skin fibroblasts were obtained by skin biopsy with informed consent. Fibroblasts derived from two non-mitochondrial disease cases were used as controls. (^{35}S) Methionine, cysteine incorporation into mitochondrially encoded proteins was analysed essentially as described previously,[18 19] using the patient's and control fibroblasts in culture. Semiconfluent cells in 6-well plates were labelled with (^{35}S) EXPRESS protein labelling mix (Perkin Elmer) for 30 min, in the presence of emetine (0.1 mg/ml) in methionine-free DMEM supplemented with dialysed 10% fetal bovine serum (FBS). The cells were lysed in 10 mM Tris-HCl (pH 7.5), 1 mM EDTA, and 1% sodium dodecyl sulfate (SDS). Total cellular proteins (10 µg/lane) were fractionated by 15–20% gradient SDS-PAGE. The gel was stained with Quick-coomassie brilliant blue (CBB) PLUS (Wako) and dried. The gel was exposed to an imaging plate, and the labelled polypeptides were located with a bioimaging analyser (BAS3000, Fuji Photo Film).

Blue native polyacrylamide gel electrophoresis (BN-PAGE) and western blotting for immunodetection[20]

Mitochondrial proteins were isolated from cultured fibroblasts from patient IV-6.[21] A mixture of mitochondrial proteins from 10 non-mitochondrial disease cases was used as a control. For the detection of individual complexes, the mitochondrial fraction (20 µg protein) was solubilised with 0.5% (w/v)

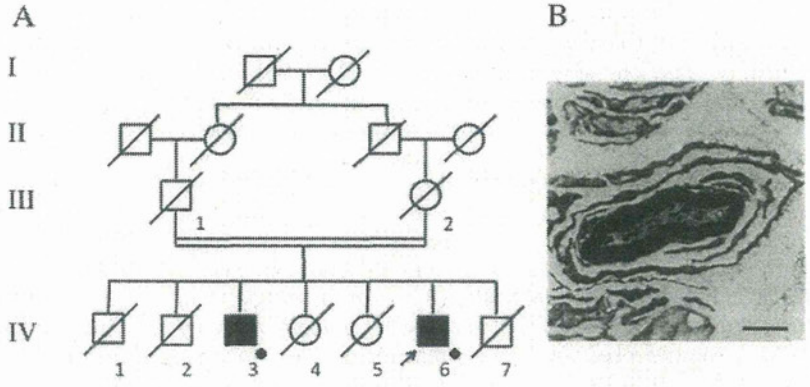

Figure 1 Family pedigree and sural nerve biopsy findings. (A) Family pedigree. The proband (IV-6) and his older brother (IV-3) show the same clinical phenotype. Other siblings are all deceased. The parents (III-1 and 2), who were first cousins, were neurologically asymptomatic before their death. Filled squares, affected males; open squares, unaffected males; open circles, unaffected females; slashes, deceased; arrow, proband; dots, examined subjects. (B) Sural nerve biopsy findings. An electron microscopic image of a sural nerve from the proband revealed the formation of an onion bulb-like structure. Bar, 2 μm.

n-dodecyl-β-D-maltoside, and for the detection of supercomplexes, the mitochondrial fraction (30 μg protein) was solubilised with 1% (w/v) digitonin, respectively. Electrophoresis was performed on 3–12% gradient polyacrylamide gels (Invitrogen).[21 22] Following BN-PAGE, the gels were blotted onto polyvinylidene fluoride membranes using an iBlot transfer system (Invitrogen). Subunit-specific primary antibodies were used to immunodetect protein complexes. The cocktail of primary antibodies comprised NDUFA9 (complex I, Invitrogen) (2.0 μg/ml), SDHA (complex II, Invitrogen) (0.02 μg/ml), UQCRC2 (complex III, Abcam) (0.2 μg/ml), MTCO1 (complex IV, Invitrogen) (0.2 μg/ml), and ATP5B (complex V, Invitrogen) (2.0 μg/ml). After removing the cocktail of primary antibodies, alkaline phosphatase-conjugated secondary antibodies were added, and then chemiluminescent detection was performed with a bioimaging system (LAS4000 mini, GE Healthcare).

Enzymatic activity of respiratory chain complexes[20]

The enzymatic activity of individual mitochondrial respiratory complexes was determined using the mitochondrial fractions (1 μg protein) isolated from cultured fibroblasts from patient IV-6 and 10 controls according to Trounce *et al*[23] with modifications. The activities of complexes I, II, III and IV were measured using a multiwell plate reader spectrophotometric system (SPECTROstar Nano, BMG Labtech). Citrate synthase (CS) activity was used for normalisation. All measurements were performed in triplicate and averaged.

RESULTS

Clinical features

The proband (IV-6) was a 32-year-old man who was admitted to our hospital for evaluation of slowly progressive weakness of the lower extremities and decreased visual acuity. He noticed the reduced visual acuity at age 7 years. At about age 10 years, his leg weakness and drop feet led to a steppage gait. He could not execute fine finger movement at age 16 years. On ophthalmologic examination, he exhibited 20/100 vision in the right eye and 20/200 in the left one. Fundoscopic examination demonstrated bilateral optic atrophy with central scotoma. On neurologic examination, bilateral leg spasticity, and anterior tibial muscle weakness and atrophy were noted. Mild distal arm weakness without atrophy was observed. Tendon reflexes,

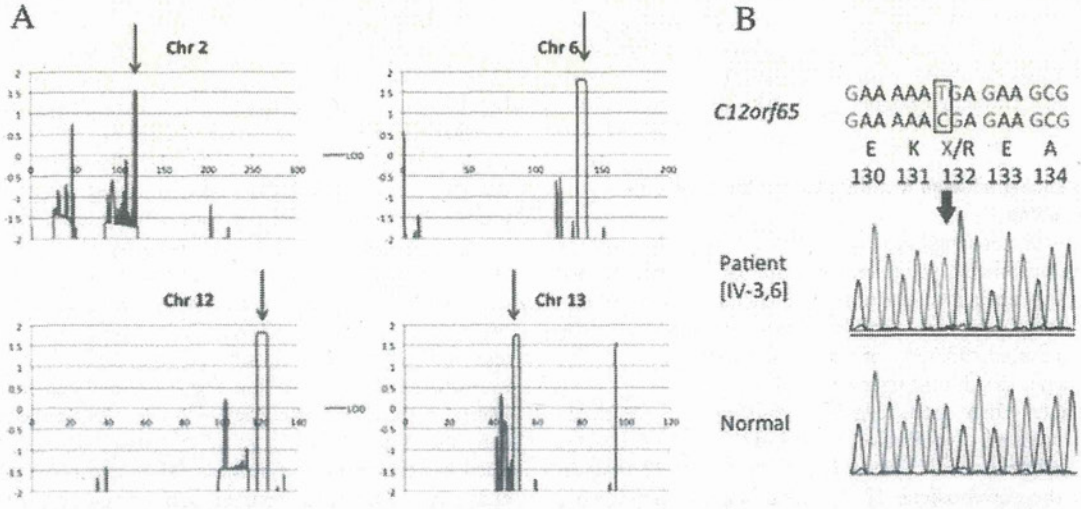

Figure 2 Linkage analysis and mutation of *C12orf65* in the proband. (A) Linkage analysis. Linkage analysis involving single nucleotide polymorphisms revealed the highest lod scores (about 1.8) in parts of chromosomes 2, 6, 12 and 13 (arrows). These four areas were thought to be candidate areas in which the causative gene was located. (B) Mutation of *C12orf65* in the proband. Sanger sequencing confirmed the homozygous nonsense mutation (c.394C>T, p.R132X9) of the C12orf65 gene identified in the proband (IV-6). The affected brother (IV-3) showed the same mutation.

except for normal ankle jerks, were exaggerated in all extremities. Bilateral planter responses were flexion. Superficial and vibratory sensations were diminished in the distal legs with a glove and stocking distribution and preserved position sense. The results of blood and cerebrospinal fluid examinations were within normal ranges. The urine organic acid pattern was normal. EEG, ECG and brain CT showed no remarkable findings. A nerve conduction study disclosed mild decreases of motor and sensory nerve conduction velocities in the upper extremities, but they were not evoked in the lower extremities. High-amplitude NMUs, and a reduced number of NMUs, were observed in the extremities on needle electromyography (EMG). Motor-evoked potential examination revealed prolongation of the central motor conduction times in the corticospinal tracts. Microscopic examination of a muscle biopsy specimen showed grouped atrophy in the tibialis anterior muscle. A sural nerve biopsy revealed a decreased number of nerve fibres of large diameter, the formation of an onion bulb-like structure, and endoneural fibrosis (figure 1B).

The second case (IV-3), a brother of the proband, exhibited essentially the same clinical phenotype. He noticed the visual difficulty at age 7 years, the onset of slowly progressive muscle atrophy in the lower extremities at age 10 years, and pes equinovarus deformities at age 12 years. Neurologic examination at age 42 years showed bilateral optic atrophy with central scotomas and diminished visual acuity (10/200 on right and 16/200 on left). In the lower extremities, marked muscular atrophy, spasticity and pes equinovarus were noted. Deep tendon reflexes were exaggerated in all extremities with left patellar clonus and extensor planter reflexes bilaterally. Superficial sensation and vibration were diminished in a glove and stocking distribution. Position sense was normal. Needle EMG showed neurogenic patterns. A nerve-conduction study disclosed slight decreases in motor nerve conduction velocities and normal sensory nerve conduction velocities in the upper extremities, but they were not evoked in the lower extremities.

Identification of candidate chromosome areas

We found linkages, that were not statistically significant, to chromosomes 2 (rs116837089-rs118552355), 6 (rs131535042-rs138306536), 12 (rs119856515-rs125250432) and 13 (rs67990237-rs70707721), with maximum cumulative logarithm of the odds (LOD) scores of 1.8 (figure 2A). Array CGH analysis revealed no pathological copy-number alterations in the four candidate chromosome areas. These four areas contained neither previously identified HSP loci nor CMT loci.

Exome sequencing allowed identification of the candidate gene substitutions

The presence of consanguinity, and the fact that the parents appeared asymptomatic, suggested that the patients had homozygous disease-causing mutations, and therefore, a homozygous autosomal-recessive model was applied. Exome sequencing covered 98.65% of the target region, and the average sequence depth on target was 41.47.

We identified three homozygous, non-synonymous single nucleotide variants (c.394C>T (p.R132X) in *C12orf65*, c.136G>A (p.E46K) in *COQ5*, and c.6599T>G (p.I2200S) in *KNTC1*) in the chromosome 12 candidate area with reference to dbSNP131. No such variations were detected in the chromosome 2, 6 and 13 areas. We could subsequently exclude the two candidate gene mutations in *COQ5* and *KNTC1* as benign polymorphisms, because the two variants had been registered as SNPs to the dbSNP134 and 1000 genomes (rs139585780: c.136G>A in *COQ5*, A allele frequency=0.0112 and rs140880563: c.6599T>G in *KNTC1*, G allele frequency=0.0056 in Japanese). The remaining candidate gene, *C12orf65*, was confirmed to have a homozygous nonsense mutation (c.394 C>T, p.R132X) on Sanger sequencing in the two patients, IV-3 and 6 (figure 2B). This nonsense mutation was not found in 200 Japanese control genomic DNAs.

Mitochondrial respiratory function is impaired by the mutation in *C12orf65*

Very recently, two homozygous *C12orf65* 1 bp deletion mutations were identified in patients with Leigh syndrome, optic atrophy and ophthalmoplegia.[24] The C12orf65 protein shows high sequence similarity to mitochondrial class I peptide release factors (RFs), and it has been reported that mutations in *C12orf65* cause a mitochondrial translation defect. Analysis of the assembly of mitochondrial phosphorylation complexes showed decreases of complexes I, III, IV and V. This disease entity is called combined oxidative phosphorylation deficiency 7 (COXPD7) (online Mendelian inheritance in man (OMIM) #613559). To determine how this nonsense mutation affects the mitochondrial function, we first performed immunoblot analysis and mitochondrial protein synthesis assaying of patient fibroblasts. Immunoblot analysis showed that a smaller C12orf65 protein was generated in the patient's fibroblasts than the wild-type protein in controls (figure 3A). Marked reductions of the synthesised polypeptides were observed in patient IV-6 compared with those in controls (16% for COX I and COX II, figure 3B), implying the aberrant statuses of respiratory complexes. Actually, complexes I and IV were severely impaired in their enzymatic functions (29% and 13%, respectively, figure 4A), and holoenzyme structures (the average value for two experiments, 17% and 23%, respectively, figure 4B) in patient IV-6, probably due to the mitochondrial translation defect, as shown in figure 3B. Furthermore, the amounts of respiratory supercomplexes that consist of complexes I, III and IV were also significantly reduced in patient IV-6 (about 30%, figure 4B). Thus, the disrupted protein integrity (function and structure) of complexes I and IV, which is closely associated with the aberrant mitochondrial bioenergetics in patient IV-6, would constitute the molecular pathogenicity in a patient carrying a mutation in *C12orf65*.

DISCUSSION

In the present study, we identified a novel *C12orf65* nonsense mutation (c.394C>T, p.R132X) in patients with spastic paraplegia with optic atrophy and neuropathy with AR inheritance (SPG55). The possibility remains that there is another undetected mutation in the four candidate chromosome areas because the exome sequencing did not cover all exons in the areas. However, our patients carried the nonsense mutation of *C12orf65* that had been identified as the causative gene for the neurological disorder COXPD7. In COXPD7, it had been reported that deletion mutations of *C12orf65* lead to a decrease in mitochondrial translation and combined oxidative phosphorylation (OXPHOS) deficiencies. In the present study, we clearly demonstrated that a nonsense mutation of *C12orf65* led to a mitochondrial protein synthesis defect and respiratory complex enzyme activity reduction, similarly. Thus, the spastic paraplegia phenotype in our patients could be a novel and distinct clinical entity based on the *C12orf65* mutation.

The C12orf65 protein is considered to belong to the mitochondrial class I peptide RFs.[24] This protein is a soluble matrix, one that is not coprecipitated with mitochondrial ribosomes,[25]

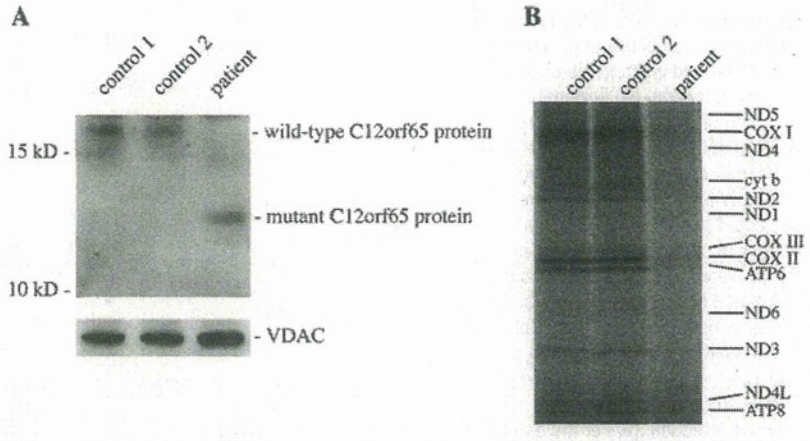

Figure 3 Immunoblot analysis of the patient's fibroblasts and mitochondrial protein synthesis assay. (A) Immunoblot analysis of the patient's fibroblasts. Immunoblot analysis of the C12orf65 protein in two controls and the patient's fibroblasts. Mitochondrial protein extracts (10 μg) were fractionated, transferred to PVDF filters, and then probed against C12orf65. VDAC was used as a loading control. Immunoblot analysis showed that a smaller C12orf65 protein (about 13 kDa) was generated in the patient's fibroblasts than the wild-type proteins (about 17 kDa) in controls. (B) Mitochondrial protein synthesis assay. Fibroblasts from a patient (IV-6) and two controls were labelled with (^{35}S) EXPRESS protein labelling mixing, and incorporated into mitochondrial encoded proteins. The fibroblasts were cultured with containing medium in the presence of emetine, as a cytosolic translation inhibitor. Total cell proteins (10 μg) were fractionated by 15–20% gradient SDS-PAGE and visualised by autoradiography. The autographic image shows the marked reduction of mitochondrial DNA translation in the patient fibroblasts compared with that in control fibroblasts. The synthesised polypeptides of combined oxidative I and II in the patient fibroblasts were reduced to 16% in density compared with those in the control fibroblasts.

and that has no peptidyl-tRNA hydrolase activity.[24] Therefore, although the actual function of C12orf65 is still not clear, it might play a role in recycling abortive peptidyl-tRNAs that have been prematurely released from ribosomes during polypeptide elongation. The nuclear C12orf65 gene comprises three exons, and its protein-coding region comprises 501 bp derived from its exons 2 and 3. The C12orf65 protein consists of 166 amino acids that include a RF-1 domain (amino acid numbers 53–146) and a glycine-glycine-glutamine (GGQ) motif (amino acid numbers 71–73). Our patients had a homozygous nonsense mutation (c.394 C>T) in exon 3, that is predicted to result in a stop codon at 132. Previously reported COXPD7 patients had two homozygous deletion mutations (c.210delA and c.248delT), and both mutations resulted in a premature stop codon at 84 in exon 2.[24]

The RT-PCR product derived from the *C12orf65* mRNA was not significantly reduced in COXPD7 patients[24] or our patients compared with that in normal controls (data not shown). We suggest that truncated C12orf65 proteins were generated in these COXPD7 and our patients (figure 3A). COXPD7 and our patients share a few clinical symptoms, that is, optic atrophy and peripheral neuropathy. We consider that our patients could be included in COXPD7 with a different clinical phenotype. However, the cardinal clinical feature in COXPD7 patients is Leigh syndrome, while that in our patients is spastic paraplegia. The former shows a more severe phenotype than the latter. We found that our patient has a relatively larger C12orf65 protein (131 amino acids) than that in COXPD7 cases (83 amino acids). Moreover, COXPD7 patient's fibroblasts have been reported to exhibit severe decreases in complexes I, IV and V. Meanwhile, our patient's fibroblasts showed decreases in complexes I and IV, and a milder decrease in complex V. In several reports, patients with mtDNA translation defects were found to be associated with an unaffected amount of complex III or a milder decrease than of other complexes.[26–29] In the case of COXPD7 patient's fibroblasts, there was a milder decrease in complex III, while our patient's fibroblasts had an unaffected amount of complex III. Therefore, our patients might have a preserved C12orf65 protein function compared with that in COXPD7.

A study involving cultured neurones showed a complex I deficiency could increase mitochondrial reactive oxygen species (ROS) production, and increase neuronal death attenuated by ROS scavengers.[30] Accumulated intracellular oxidative damage to neurones could be a causative mechanism for neurodegeneration caused by mitochondrial respiratory deficiencies.

To date, several HSP genes related to mitochondria have been identified: *paraplegin* and *HSPD1*. The SPG31 protein, receptor expression-enhancing protein 1 (REEP1), coordinates ER shaping and microtubule dynamics,[31] although another report has proposed that REEP1 is a mitochondrial protein.[32] SPG7 is an AR-complicated HSP resulting from *paraplegin* gene mutations. The clinical features of SPG7 are varied with associated symptoms: cerebellar signs, optic atrophy, distal amyotrophy

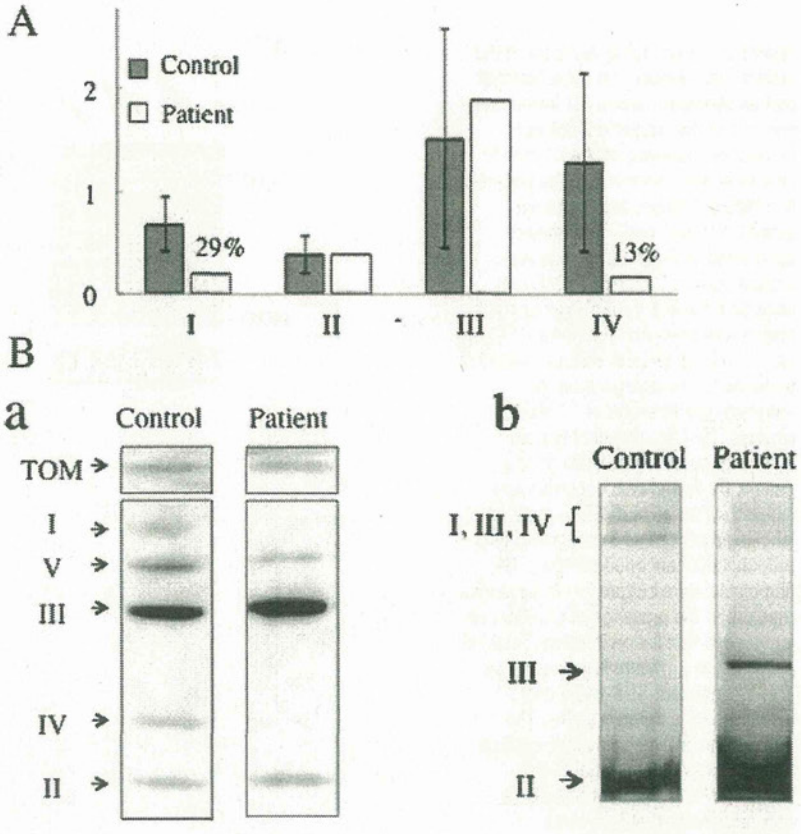

Figure 4 Enzymatic activities of respiratory complexes, and blue native polyacrylamide gel electrophoresis (BN-PAGE) and western blotting for immunodetection. (A) Enzymatic activities of respiratory complexes. Isolated mitochondrial fractions (1 μg protein) of cultured fibroblasts from patient IV-6 and 10 controls were subjected to spectrophotometry. The activity of citrate synthase was used for normalisation. All measurements were performed in triplicate and averaged. The enzymatic activities of complexes I and IV were severely decreased (29% and 13%, respectively). (B). BN-PAGE and western blotting for immunodetection. (a) For the detection of individual complexes, isolated mitochondrial fractions (20 μg protein) were solubilised with 0.5% (w/v) *n*-dodecyl-β-D-maltoside, and then electrophoresed on 3–12% gradient polyacrylamide gels. The subunit-specific primary antibodies used were as follows: NDUFA9 (complex I, Invitrogen) (2.0 μg/ml), SDHA (complex II, Invitrogen) (0.02 μg/ml), UQCRC2 (complex III, Abcam) (0.2 μg/ml), MTCO1 (complex IV, Invitrogen) (0.2 μg/ml), and ATP5B (complex V, Invitrogen) (2.0 μg/ml). Translocase of the outer membrane was used as the loading control. Immunoblot images show that the amounts of complexes I and IV were decreased to about 11% and 21% in patient IV-6. (b) For the detection of supercomplexes, isolated mitochondrial fractions (30 μg protein) were solubilised with 1% (w/v) digitonin, and then electrophoresed on 3–12% gradient polyacrylamide gels. The subunit-specific primary antibodies used were as follows: SDHA (complex II, Invitrogen) (0.02 μg/ml) and UQCRC2 (complex III, Abcam) (0.2 μg/ml). Immunoblot images show that the amounts of supercomplexes that consist of complexes I, III and IV were also reduced to about 30% in patient IV-6.

and peripheral neuropathy. Our patients and SPG7 ones share the symptoms of optic atrophy and neuropathy as well as spastic paraplegia, although the *paraplegin* gene mutation was not identified in this family.

Paraplegin is a nuclear-encoded mitochondrial protein. SPG7 fibroblasts have been demonstrated to exhibit reduced respiratory chain complex I activity.[33] Complex I activity was also reduced in our patient's fibroblasts. Considering the above findings, the present type of HSP has some clinical and biochemical features in common with SPG7. Furthermore, there has been one report of a defect of complex I activity in HSP patients without SPG7 gene mutations,[34] and another one with significant decreases in mitochondrial respiratory chain complexes I and IV in non-SPG4/SPG7 HSP families.[35] These families might have a mutation in the *C12orf65* genes responsible for reduced mitochondrial respiratory chain complex activities.

It may be noteworthy that in Friedreich's ataxia (FA), another nuclear-encoded mitochondrial defect, there is corticospinal degeneration. In rare cases, FA may present clinically as spastic paraparesis.[36 37]

In conclusion, the present study allowed identification of a *C12orf65* gene mutation in AR-HSP with optic atrophy and neuropathy, and revealed a mitochondrial translation dysfunction resulting in reduced enzyme activities of respiratory chain

complexes. Our study should provide additional insights into the pathogeneses of HSPs or other neurodegenerative diseases involving mitochondrial gene mutations.

Acknowledgements We wish to thank Dr Mayumi Komine (Department of Dermatology, Jichi Medical University) for performing the skin biopsy on the patient. We also thank Dr Satoko Kumada (Department of Neuropediatrics, Tokyo Metropolitan Neurological Hospital) and Dr Kazuma Sugie (Department of Neurology, Nara Medical University) for sending the patients' samples.

Contributors HS, YT, JG, ST and YG designed the study; HS, HI, CS, YM, HH, JH, KS, TN, MN, YF and YT performed the experiments; HS, YT, HI, CS, YM, HH, JG, ST and YG collected and analysed the data; HS provided the DNA samples and clinical information; HS, YT, ST and YG wrote the manuscript; and YT, JG, ST, YG and IH provided technical support, conceptual advice and project coordination.

Funding This work was supported by a grant from the Research Committee for Ataxic Diseases (YT and HS) of the Ministry of Health, Labour and Welfare, Japan. This work was also supported by Grants-in-Aid from the Research Committee of CNS Degenerative Diseases (IN and YT), and the Ministry of Health, Labour and Welfare of Japan, and by a Grant-in-Aid for Scientific Research (C) (23591253 to HS) from The Ministry of Education, Culture, Sports, Science and Technology in Japan.

Competing interests None.

Patient consent Obtained.

Ethics approval This study was approved by the institutional review board of the Jichi Medical University, University of Yamanashi, University of Tokyo, and the National Institute of Neuroscience, National Centre of Neurology and Psychiatry.

Provenance and peer review Not commissioned; externally peer reviewed.

Data sharing statement Exome sequencing data are available (DDBJ Sequence Read Archive (DRA) accession number DRA000534).

REFERENCES

1. **Harding AE.** Classification of the hereditary ataxias and paraplegias. *Lancet* 1983;**1**:1151–5.
2. **Hazan J,** Fonknechten N, Mavel D, Paternotte C, Samson D, Artiguenave F, Davoine CS, Cruaud C, Durr A, Wincker P, Brottier P, Cattolico L, Barbe V, Burgunder JM, Prud'homme JF, Brice A, Fontaine B, Heilig B, Weissenbach J. Spastin, a new AAA protein, is altered in the most frequent form of autosomal dominant spastic paraplegia. *Nat Genet* 1999;**23**:296–303.
3. **Stevanin G,** Santorelli FM, Azzedine H, Coutinho P, Chomilier J, Denora PS, Martin E, Ouvrard-Hernandez AM, Tessa A, Bouslam N, Lossos A, Charles P, Loureiro JL, Elleuch N, Confavreux C, Cruz VT, Ruberg M, Leguern E, Grid D, Tazir M, Fontaine B, Filla A, Bertini E, Durr A, Brice A. Mutations in SPG11, encoding spatacsin, are a major cause of spastic paraplegia with thin corpus callosum. *Nat Genet* 2007;**39**:366–72.
4. **Salinas S,** Proukakis C, Crosby A, Warner TT. Hereditary spastic paraplegia: clinical features and pathogenetic mechanisms. *Lancet Neurol* 2008;**7**:1127–38.
5. **McDermott CJ,** Grierson AJ, Wood JD, Bingley M, Wharton SB, Bushby KM, Shaw PJ. Hereditary spastic paraparesis: disrupted intracellular transport associated with spastin mutation. *Ann Neurol* 2003;**54**:748–59.
6. **Xia CH,** Roberts EA, Her LS, Liu X, Williams DS, Cleveland DW, Goldstein LS. Abnormal neurofilament transport caused by targeted disruption of neuronal kinesin heavy chain KIF5A. *J Cell Biol* 2003;**161**:55–66.
7. **Tarrade A,** Fassier C, Courageot S, Charvin D, Vitte J, Peris L, Thorel A, Mouisel E, Fonknechten N, Roblot N, Seilhean D, Dierich A, Hauw JJ, Melki J. A mutation of spastin is responsible for swellings and impairment of transport in a region of axon characterized by changes in microtubule composition. *Hum Mol Genet* 2006;**15**:3544–58.
8. **Koppen M,** Metodiev MD, Casari G, Rugarli EI, Langer T. Variable and tissue-specific subunit composition of mitochondrial m-AAA protease complexes linked to hereditary spastic paraplegia. *Mol Cell Biol* 2007;**27**:758–67.
9. **Nolden M,** Ehses S, Koppen M, Bernacchia A, Rugarli EI, Langer T. The m-AAA protease defective in hereditary spastic paraplegia controls ribosome assembly in mitochondria. *Cell* 2005;**123**:277–89.
10. **Pierson TM,** Adams D, Bonn F, Martinelli P, Cherukuri PF, Teer JK, Hansen NF, Cruz P, Mullikin JC, Blakesley RW, Golas G, Kwan J, Sandler A, Fuentes Fajardo K, Markello T, Tifft C, Blackstone C, Ruqarli EI, Langer T, Gahl WA, Toro C For The Nisc Comparative Sequencing Program. Whole-exome sequencing identifies homozygous AFG3L2 mutations in a spastic ataxia-neuropathy syndrome linked to mitochondrial m-AAA proteases. *PLoS Genet* 2011;**7**:e1002325.
11. **Ferreirinha F,** Quattrini A, Pirozzi M, Valsecchi V, Dina G, Broccoli V, Auricchio A, Piemonte F, Tozzi G, Gaeta L, Casari G, Ballabio A, Rugarli EI. Axonal degeneration in paraplegin-deficient mice is associated with abnormal mitochondria and impairment of axonal transport. *J Clin Invest* 2004;**113**:231–42.
12. **Joshita Y,** Atsumi T, Miyatake T. Two siblings with spastic paraplegia, optic atrophy and peripheral neuropathy. *Rinsho Shinkeigaku* 1982;**22**:901–8.
13. **Fukuda Y,** Nakahara Y, Date H, Takahashi Y, Goto J, Miyashita A, Kuwano R, Adachi H, Nakamura E, Tsuji S. SNP HiTLink: a high-throughput linkage analysis system employing dense SNP data. *BMC Bioinformatics* 2009;**10**:121.
14. **Gudbjartsson DF,** Thorvaldsson T, Kong A, Gunnarsson G, Ingolfsdottir A. Allegro version 2. *Nature Genet* 2005;**37**:1015–16.
15. **Barrett MT,** Scheffer A, Ben-Dor A, Sampas N, Lipson D, Kincaid R, Tsang P, Curry B, Baird K, Meltzer PS, Yakhini Z, Bruhn L, Laderman S. Comparative genomic hybridization using oligonucleotide microarrays and total genomic DNA. *Proc Natl Acad Sci USA* 2004;**101**:17765–70.
16. **Mitsui J,** Takahashi Y, Goto J, Tomiyama H, Ishikawa S, Yoshino H, Minami N, Smith DI, Lesage S, Aburatani H, Nishino I, Brice A, Hattori N, Tsuji S. Mechanisms of genomic instabilities underlying two common fragile-site-associated loci, PARK2 and DMD, in germ cell and cancer cell lines. *Am J Hum Genet* 2010;**87**:75–89.
17. **Matsushima Y,** Adan C, Garesse R, Kaguni LS. Drosophila mitochondrial transcription factor B1 modulates mitochondrial translation but not transcription or DNA copy number in Schneider cells. *J Biol Chem* 2005;**280**:16815–20.
18. **Chomyn A,** Meola G, Bresolin N, Lai ST, Scarlato G, Attardi G. In vitro genetic transfer of protein synthesis and respiration defects to mitochondrial DNA-less cells with myopathy-patient mitochondria. *Mol Cell Biol* 1991;**11**:2236–44.
19. **Hayashi JI,** Ohta S, Takai D, Miyabayashi S, Sakuta R, Goto Y, Nonaka I. Accumulation of mtDNA with a Mutation at Position 3271 in tRNALeu(UUR) Gene Introduced from a Melas Patient to HeLa Cells Lacking mtDNA Results in Progressive Inhibition of Mitochondrial Respiratory Function. *Biochem Biophys Res Commun* 1993;**197**:1049–55.
20. **Mimaki M,** Hatakeyama H, Komaki H, Yokoyama M, Arai H, Kirino Y, Suzuki T, Nishino I, Nonaka I, Goto Y. Reversible infantile respiratory chain deficiency: a clinical and molecular study. *Ann Neurol* 2010;**68**:845–54.
21. **Nijtmans LG,** Henderson NS, Holt IJ. Blue Native electrophoresis to study mitochondrial and other protein complexes. *Methods* 2002;**26**:327–34.
22. **D'Aurelio M,** Gajewski CD, Lenaz G, Manfredi G. Respiratory chain supercomplexes set the threshold for respiration defects in human mtDNA mutant cybrids. *Hum Mol Genet* 2006;**15**:2157–69.
23. **Trounce LA,** Kim YL, Jun AS, Wallace DC. Assessment of mitochondrial oxidative phosphorylation in patient muscle biopsies, lymphoblasts, and transmitochondrial cell lines. In: Attardi GM, Chomyn A eds. *Methods in enzymology*. Vol. 264. San Diego: Academic Press USA, 1996:484–509.
24. **Antonicka H,** Ostergaard E, Sasarman F, Weraarpachai W, Wibrand F, Pedersen AM, Rodenburg RJ, van der Knaap MS, Smeitink JA, Chrzanowska-Lightowlers ZM, Shoubridge EA. Mutations in C12orf65 in patients with encephalomyopathy and a mitochondrial translation defect. *Am J Hum Genet* 2010;**87**:115–22.
25. **Richter R,** Rorbach J, Pajak A, Smith PM, Wessels HJ, Huynen MA, Smeitink JA, Lightowlers RN, Chrzanowska-Lightowlers ZM. A functional peptidyl-tRNA hydrolase, ICT1, has been recruited into the human mitochondrial ribosome. *EMBO J* 2010;**29**:1116–25.
26. **Smeitink JA,** Elpeleq O, Antonicka H, Diepstra H, Saada A, Smits P, Sasarman F, Vriend G, Jacob-Hirsch J, Shaaq A, Rechavi G, Welling B, Horst J, Rodenburg RJ, van den Heuvel B, Shoubridge EA. Distinct clinical phenotypes associated with a mutation in the mitochondrial translation elongation factor EFTs. *Am J Hum Genet* 2006;**79**:869–77.
27. **Fornuskova D,** Brantova O, Tesarova M, Stiburek L, Honzik T, Wenchich L, Tietzeova E, Hansikova H, Zeman J. The impact of mitochondrial tRNA mutations on the amount of ATP synthase differs in the brain compared to other tissues. *Biochem Biophys Acta* 2008;**1782**:317–25.
28. **Smits P,** Antonicka H, van Hasselt PM, Weraarpachai W, Haller W, Schreurs M, Venselaar H, Rodenburg RJ, Smeitink JA, van den Heuvel LP. Mutation in subdomain G' of mitochondrial elongation factor G1 is associated with combined OXPHOS deficiency in fibroblasts but not in muscle. *Eur J Hum Genet* 2011;**19**:275–9.
29. **Smits P,** Saada A, Wortmann SB, Heister AJ, Brink M, Pfundt R, Miller C, Haas D, Hantschmann R, Rodenburg RJ, Smeitink JA, van den Heuvel LP. Mutation in mitochondrial ribosomal protein MRPS22 leads to Cornelia de Lange-like phenotype, brain abnormalities and hypertrophic cardiomyopathy. *Eur J Hum Genet* 2011;**19**:394–9.
30. **Abramov AY,** Smulders-Srinivasan TK, Kirby DM, Acin-Perez R, Enriquez JA, Lightowlers RN, Duchen MR, Turnbull DM. Mechanism of neurodegeneration of neurons with mitochondrial DNA mutations. *Brain* 2010;**133**:797–807.
31. **Park SH,** Zhu PP, Parker RL, Blackstone C. Hereditary spastic paraplegia proteins REEP1, spastin, and atlastin-1 coordinate microtubule interactions with the tubular ER network. *J Clin Invest* 2010;**120**:1097–110.
32. **Zuchner S,** Wang G, Tran-Viet KN, Nance MA, Gaskell PC, Vance JM, Ashley-Koch AE, Pericak-Vance MA. Mutations in the novel mitochondrial protein REEP1 cause hereditary spastic paraplegia type 31. *Am J Hum Genet* 2006;**79**:365–9.
33. **Atorino L,** Silvestri L, Koppen M, Cassina L, Ballabio A, Marconi R, Langer T, Casari G. Loss of m-AAA protease in mitochondria causes complex I deficiency and increased sensitivity to oxidative stress in hereditary spastic paraplegia. *J Cell Biol* 2003;**163**:777–87.
34. **Piemonte F,** Casali C, Carrozzo R, Schagger H, Patrono C, Tessa A, Tozzi G, Cricchi F, Di Capua M, Siciliano G, Amabile GA, Morocutti C, Bertini E, Santorelli FM.

Respiratory chain defects in hereditary spastic paraplegias. *Neuromuscul Disord* 2001;**11**:565–9.

35. **McDermott CJ,** Taylor RW, Hayes C, Johnson M, Bushby KM, Turnbull DM, Shaw PJ. Investigation of mitochondrial function in hereditary spastic paraparesis. *Neuroreport* 2003;**14**:485–8.
36. **Castelnovo G,** Biolsi B, Barbaud A, Labauge P, Schmitt M. Isolated spastic paraparesis leading to diagnosis of Friedreich's ataxia. *J Neurol Neurosurg Psychiatry* 2000;**69**:693.
37. **Wilkinson PA,** Bradley JL, Warner TT. Friedreich's ataxia presenting as an isolated spastic paraparesis. *J Neurol Neurosurg Psychiatry* 2001;**71**:707–10.

A homozygous mutation of *C12orf65* causes spastic paraplegia with optic atrophy and neuropathy (SPG55)

Haruo Shimazaki, Yoshihisa Takiyama, Hiroyuki Ishiura, et al.

J Med Genet 2012 49: 777-784
doi: 10.1136/jmedgenet-2012-101212

Neurogenetics (2012) 13:237–243
DOI 10.1007/s10048-012-0330-0

ORIGINAL ARTICLE

Clinical features and haplotype analysis of newly identified Japanese patients with gelsolin-related familial amyloidosis of Finnish type

Makiko Taira · Hiroyuki Ishiura · Jun Mitsui · Yuji Takahashi · Toshihiro Hayashi · Jun Shimizu · Takashi Matsukawa · Naoko Saito · Kazumasa Okada · Sadatoshi Tsuji · Hiromasa Sawamura · Shiro Amano · Jun Goto · Shoji Tsuji

Received: 1 March 2012 / Accepted: 16 April 2012 / Published online: 24 May 2012

Abstract Familial amyloidosis of the Finnish type (FAF) is an autosomal dominant form of systematic amyloidosis characterized by lattice corneal dystrophy, cranial neuropathy, and *cutis laxa*. Although FAF has been frequently found in the Finnish population, FAF is a considerably rare disorder in other regions. In this study, we examined the clinical characteristics as well as the haplotypes of six Japanese patients with FAF from five families. They showed the typical clinical presentations of FAF, but we found a broad range of ages at onset of neurological symptoms. All members had the c.654G>A mutation in *GSN*. To evaluate the disease haplotypes, high-density single-nucleotide polymorphism (SNP) arrays were used and disease-relevant haplotypes were reconstructed. Haplotype analysis in the four apparently unrelated families suggested a common founder haplotype. In a sporadic FAF patient, however, the haplotype was dissimilar to the founder haplotype. The present study demonstrated that a founder mutation in most of the Japanese families with FAF, except for a sporadic patient in whom a *de novo* mutation event was suggested as the origin of the mutation.

Keywords Gelsolin-related familial amyloidosis · Haplotype analysis · SNP typing

Electronic supplementary material The online version of this article (doi:10.1007/s10048-012-0330-0) contains supplementary material, which is available to authorized users.

M. Taira · H. Ishiura · J. Mitsui · Y. Takahashi · T. Hayashi · J. Shimizu · T. Matsukawa · N. Saito · J. Goto · S. Tsuji
Department of Neurology, Graduate School of Medicine, The University of Tokyo, 7-3-1, Hongo, Bunkyo-ku, Tokyo 113-8655, Japan

K. Okada · S. Tsuji
Department of Neurology, School of Medicine, University of Occupational and Environmental Health, 1-1, Iseigaoka, Yahatanishi-ku, Kitakyushu 807-8555, Japan

H. Sawamura · S. Amano
Department of Ophthalmology, Graduate School of Medicine, The University of Tokyo, 7-3-1, Hongo, Bunkyo-ku, Tokyo 113-8655, Japan

S. Tsuji (✉)
Medical Genome Center, The University of Tokyo Hospital, 7-3-1, Hongo, Bunkyo-ku, Tokyo 113-8655, Japan
e-mail: tsuji@m.u-tokyo.ac.jp

Introduction

Familial amyloidosis of the Finnish type (FAF) is an autosomal dominant form of systemic amyloidosis, which was first described in Finland [1]. FAF is clinically characterized by lattice corneal dystrophy, progressive cranial and peripheral neuropathy, and *cutis laxa* [1]. In some patients, renal and cardiac manifestations are observed [2]. It has been reported that lattice corneal dystrophy can be observed in patients as early as in their second decade, and cranial neuropathy appears gradually after their third decade [2].

The amyloid fibril protein in FAF is composed of gelsolin, an actin-modulating protein [3]. Two missense mutations in the gelsolin gene (*GSN*) on chromosome 9q33.2 have been identified as the causative mutations. The c.654G>A transition substituting Asn for Asp at codon 187 is the first and most common mutation identified in patients with FAF. This mutation has been identified in all

the Finnish patients [4–9]. Interestingly, the same mutation has also been identified in the Japanese patients [10–17] as well as in affected American [4, 5, 18, 19], Spanish [20], French [2], Dutch [21], Portuguese [22], British [23], and Iranian [24, 25] families. The second mutation is the c.654G>T transversion leading to a p.Asp187Tyr substitution and was found only in affected French, Danish, Czech, and Brazilian families [2, 4, 5, 26] with similar clinical manifestations.

A marked clustering of FAF has been observed in Southern Finland [27]. The number of disease carriers in the Finnish population has been estimated to be as many as 1,000 [28]. In Finnish patients, the existence of a strong founder effect has been demonstrated by haplotype analysis [29].

To date, eight Japanese families with FAF have been described, and intriguingly, all the patients carry the c.654G>A mutation, raising the possibility of a founder effect in the Japanese FAF mutation as well. A previous study revealed that two Japanese FAF families shared a common haplotype, but the haplotype associated with the two Japanese families was different from that associated with Finnish families [29]. In that previous study, however, only two families originating from neighboring regions were recruited, and a limited number of DNA markers were used. Thus, a more detailed analysis of the haplotypes associated with Japanese FAF patients is required to confirm whether a strong founder effect is present in the Japanese FAF patients.

In this study, we conducted a clinical examination of six patients with FAF including newly identified patients from different regions of Japan. Furthermore, to investigate the possibility of a founder mutation in these patients, we conducted detailed haplotype analysis employing microsatellites and high-density single-nucleotide polymorphism (SNP) markers.

Subjects and methods

Patients and families

Six FAF patients (III-6 and IV-4 of Family1, II-1 of Family 2, II-5 of Family 3, III-12 in Family 4, and III-4 in Family 5, shown as the dots in Fig. 1a) were enrolled in this study. Individual III-12 of Family 4 was a descendant of a family that was already reported previously [15]. Clinical information of individuals III-6 of Family 1 [16] and II-5 of Family 3 [10] was partly reported previously. Molecular investigations were performed after written informed consent was obtained from all the participating family members. The study was approved by the institutional review board of The University of Tokyo.

Mutational analysis of *GSN*

Genomic DNAs were extracted from peripheral blood leukocytes in accordance with standard procedures. Exon 4 of *GSN* was amplified using flanking intronic primers (Supplementary Table 1). Direct nucleotide sequence analysis was performed using ExoSAP-IT (USB, Cleveland, OH), a BigDye Terminator v3.1 kit, and XTerminator employing an ABI PRISM3100 sequencer (Life Technologies Corporation, Carlsbad, CA).

Haplotype analysis

To determine the disease-associated haplotypes, high-density SNP typing was carried out in the six individuals (Fig. 1a), employing Genome-Wide Human SNP array 6.0 in accordance with the manufacturer's instructions (Affymetrix, Santa Clara, CA). The genotype of each individual was determined using Genotyping Console 4.0 (Affymetrix). Haplotypes were reconstructed manually by minimizing the number of recombination events. When the genotypes of the other family members were unavailable, we determined homozygosity haplotypes [30], employing SNPs with minor allele frequencies (MAF)>5 %. In the six individuals and additional four individuals indicated by stars in Fig. 1a, we analyzed five microsatellite markers near *GSN* (GSN, D9S103, AFMa061xd9, AFMa139xb9, and D9S282) that have been analyzed in a previous study (Supplementary Table 1) [29]. Allele frequencies of SNPs were obtained from HapMap-JPT data. Linkage disequilibrium (LD) data of HapMap-JPT and HapMap-CHB were used in this study (http://www.hapmap.org/).

Results

Clinical presentations of newly identified patients

Family 1

The proband (III-6) noted bilateral blepharoptosis at the age of 57 followed by the appearance of dysarthria and a small voice. Blepharoptosis was retrospectively evident from old pictures taken when the patient was approximately 30 years of age. At the age of 61, the patient started to have dysphagia. On examination at the age of 61, blepharoptosis, facial weakness, dysarthria, dysphagia, tongue atrophy and fasciculations, and distal dysesthesia in the extremities as well as *cutis laxa* and lattice corneal dystrophy were observed. At that time, the molecular diagnosis of FAF was made [16]. At the age of 70, blepharoplasty (levator resection) was performed. From the age of 73, the patient had severe dysarthria and began to write messages to communicate with

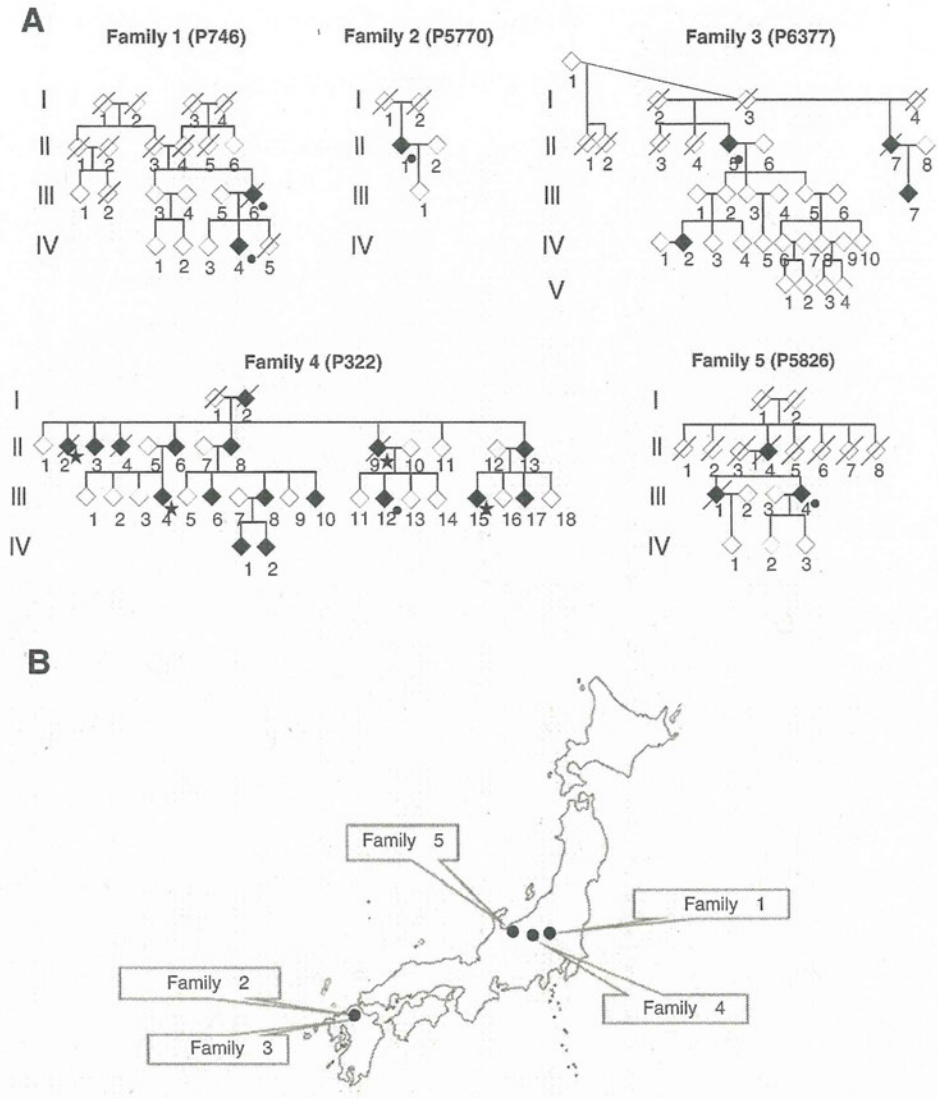

Fig. 1 Pedigree chart of Japanese families with FAF. **a** Affected individuals are indicated with *filled symbols*. *Symbols with a line* indicate deceased individuals. Individuals indicated by *dots* are clinically investigated in the study and are genotyped using dense single-nucleotide polymorphism and microsatellite markers. Microsatellite markers are also genotyped in individuals indicated by *stars*. For confidentiality purposes gender is not indicated. **b** The residences of the families are shown

others. The patient died of a malignancy at the age of 76, at which age when restricted eye movement was observed. The offspring (IV-4) was found to have lattice corneal dystrophy at the age of 28, but did not have any neurological symptoms at the age of 43.

Family 2

II-1 noted bilateral blepharoptosis at the age of 67. At the age of 77, the patient consulted an ophthalmologist for progressive loss of visual acuity, who pointed out cataract and lattice corneal dystrophy. Because facial weakness and masseter weakness were also observed, the clinical diagnosis of FAF was made. On examination at the age of 78, the patient became aware of hypesthesia at the distal portion of the extremities, although the patient did not show weakness in the extremities. The patient"s tendon reflexes were attenuated. There were no other affected individuals in this family. The father and mother of the patient died without any symptoms indicative of FAF at the ages of 85 and 97, respectively.

Family 3

II-5 noted decreased sweating at the age of approximately 40 years. Neurological examination at the age of 70 revealed facial weakness, hypoglossal nerve palsy, distal paresthesia, and autonomic dysfunction [10]. At the age of 87, bulbar palsy including dysphagia progressed, but limb weakness was not evident.

Family 4

III-12 complained of blepharoptosis, progressive facial weakness, dysesthesia around the mouth, dysarthria, and mild paresthesia of extremities at the age of 55. Decreased tendon

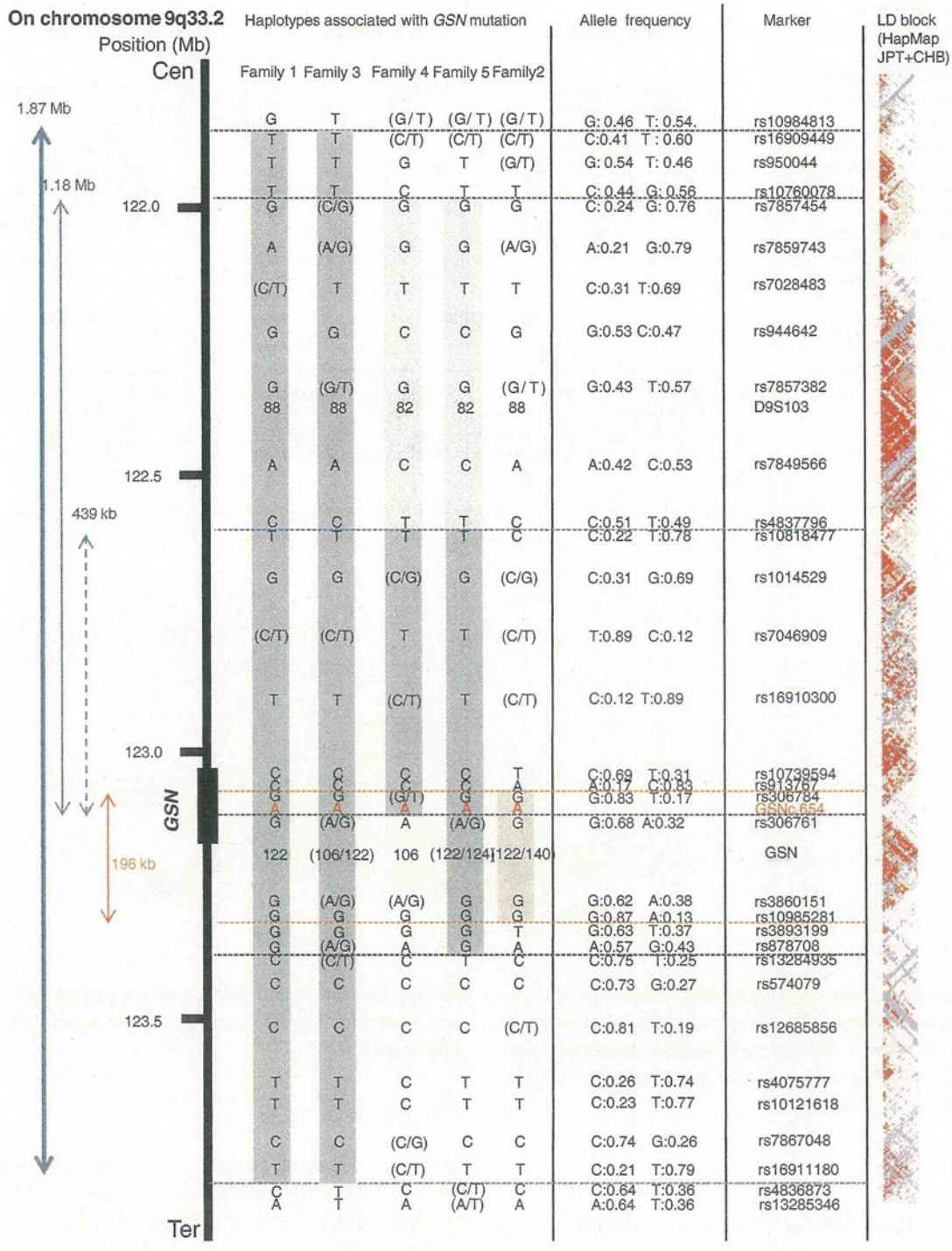

Fig. 2 FAF-relevant haplotypes of five families. FAF-relevant haplotypes around a *GSN* locus constructed using SNPs and microsatellite markers are shown. Allele frequencies of SNPs used and LD blocks of HapMap JPT+CHB samples are indicated. Families 1 and 3 shared a substantially large region of 1.87 Mb in their FAF-relevant haplotypes with the centromeric and telomeric boundaries defined by rs16909449 and rs16911180, respectively (*blue thick line*). Families 4 and 5 also shared a common haplotype of 1.11 Mb defined by rs7857454 and *GSN* c.654 (*blue line*). When the shared haplotype of Families 4 and 5 is compared with that of Families 1 and 3, it is evident that a haplotype of 439 kb defined by rs10818477 and *GSN* c.654 is commonly shared by these four families (*dotted blue line*). However, Family 2 shares only a small segment of 196 kb at most with Families 1, 3, 4, and 5 with the centromeric and telomeric boundaries defined by rs306784 and rs1098528, respectively (*red arrow*)

reflexes in the extremities and lattice corneal dystrophy were also observed, but the patient did not show cutis laxa.

Family 5

III-4 detected facial weakness and blepharoptosis at the age of 70. From the age of 75, the patient started to show weakness of the extremities. On examination at the age of 80, abducens nerve palsy, atrophy of the masseter muscle, and decreased deep sensation in the lower extremities were noted. Lattice corneal dystrophy and *cutis laxa* were also present. Skin biopsy showed amyloid deposition around sweat glands as well as vascular vessels.

The residences of the five families are summarized in Fig. 1b.

Mutational analysis

Mutational analysis of *GSN* confirmed that all six patients had the c.654G>A (p.Asp187Asn) mutation.

Haplotype analysis

The haplotypes of the five families were constructed employing dense SNPs and microsatellite markers (Fig. 2). Families 1 and 3 shared a substantially large region of 1.87 Mb in their FAF-relevant haplotypes with the centromeric and telomeric boundaries defined by rs16909449 and rs16911180, respectively. Families 4 and 5 also shared a common haplotype of 1.11 Mb defined by rs7857454 and *GSN c.654G>A*. These four families shared a 439-kb segment of the haplotypes. In contrast, the patient with sporadic FAF in Family 2 only shared a 196-kb segment of the haplotype at most defined by rs306784 and rs10985281 with those of Families 1, 3, 4, and 5, which contained only two haploblocks.

When the boundaries of the individual disease-relevant haplotypes and the haploblocks obtained by LD analysis were compared, findings suggest that the boundaries are localized to the boundaries of the haploblocks (Fig. 2), indicating that haplotype boundaries are associated with high recombination events.

Discussion

In this study, we found that all the patients in the five families carry the p.Asp187Asn mutation (c.654G>A) in *GSN* which is the same mutation as that found in the Japanese FAF patients in previous studies [10–17]. The clinical presentations of our patients included *cutis laxa*, lattice corneal dystrophy, and multiple cranial neuropathies. Blepharoptosis and facial weakness were the most common neurological findings among the patients. Weakness of the masseter muscle and weakness of the extremities were observed in two of the four patients aged over 70, suggesting that masseter weakness and extremity weakness are late manifestations. Notably, the disease onset of III-4 of Family 5 was substantially late (in the 70s). Analysis of the clinical information on the patients in the literature and those enrolled in this study revealed that the ages at onset of the initial clinical symptoms are broadly distributed between the first and the seventh decades, while cranial neuropathies are later manifestations with the age at onset distributed between the 40s and 70s (Fig. 3a). These observations suggest that the distribution of ages at onset is substantially broad despite all the patients sharing the same mutation.

Because we found the same mutation in all the patients, we then carried out haplotype analysis to explore the possibility of a founder mutation. The four apparently unrelated

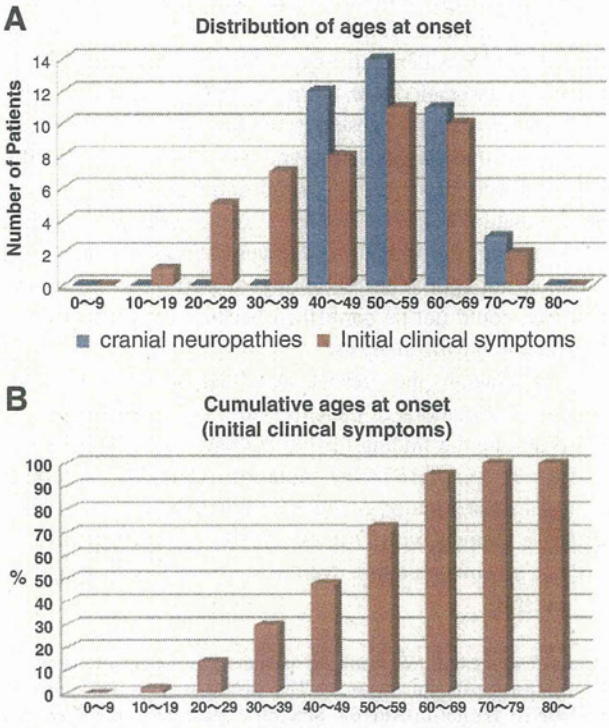

Fig. 3 Ages at onset of clinical symptoms of FAF patients and cumulative ages at onset. **a** Distribution of the ages at onset of the FAF patients with the heterozygous p.Asp187Asn mutation described in the literature [4, 8, 10–19, 22, 24, 31, 32–36] and those of the patients described in this study are shown. The distribution of ages at onset of initial clinical symptoms associated with FAF is shown by *red bars* and that of cranial neuropathies is shown by *blue bars*. **b** The cumulative age at onset of the initial clinical symptoms associated with FAF in all the patients with the heterozygous p.Asp187Asn mutation described in the literature (n=38) [4, 8, 10–19, 22, 24, 31, 32–36] and those of the patients described in this study (n=6). The analysis shows that 72.7 % of the patients develop symptoms by 50s, 95.4 % by 60s, and all the patients by 70s, indicating that the heterozygous p.Asp187Asn mutation is completely penetrant by 70s